Author Manuscript

Author Manuscript

Author Manuscript

Author Manuscript

HHS Public Access

Author manuscript

Glia. Author manuscript; available in PMC 2019 October 01.

Published in final edited form as:

Glia. 2018 October ; 66(10): 2137–2157. doi:10.1002/glia.23467.

Prokineticin-2 promotes chemotaxis and alternative A2 reactivity of astrocytes

Matthew Neal[1], **Dan Luo**[1], **Dilshan S. Harischandra**[1], **Richard Gordon**[1], **Souvarish Sarkar**[1], **Huajun Jin**[1], **Vellareddy Anantharam**[1], **Laurent Désaubry**[2], **Anumantha Kanthasamy**[1], and **Arthi Kanthasamy**[1]

[1]Parkinson Disorders Research Program, Iowa Center for Advanced Neurotoxicology, Department of Biomedical Sciences, Iowa State University, Ames, Iowa 50011

[2]Therapeutic Innovation Laboratory (UMR7200), CNRS-University of Strasbourg, Illkirch, France

Abstract

Astrocyte reactivity is disease- and stimulus-dependent, adopting either a pro-inflammatory A1 phenotype or a protective, anti-inflammatory A2 phenotype. Recently, we demonstrated, using cell culture, animal models and human brain samples, that dopaminergic neurons produce and secrete higher levels of the chemokine-like signaling protein Prokineticin-2 (PK2) as a compensatory protective response against neurotoxic stress. Since astrocytes express a high level of PK2 receptors, herein, we systematically characterize the role of PK2 in astrocyte structural and functional properties. PK2 treatment greatly induced astrocyte migration, which was accompanied by a shift in mitochondrial energy metabolism, a reduction in pro-inflammatory factors, and an increase in the anti-oxidant genes *Arginase-1* and *Nrf2*. Overexpression of PK2 in primary astrocytes or in the *in vivo* mouse brain induced the A2 astrocytic phenotype with upregulation of key protective genes and A2 reactivity markers including *Arginase-1* and *Nrf2*, *PTX3*, *SPHK1* and *TM4SF1*. A small molecule PK2 agonist IS20 not only mimicked the protective effect of PK2 in primary cultures, but also increased glutamate uptake by upregulating GLAST. Notably, IS20 blocked not only MPTP-induced reductions in the A2 phenotypic markers SPHK1 and SCL10a6 but also elevation of the of A1 marker GBP2. Collectively, our results reveal that PK2 regulates a novel neuron-astrocyte signaling mechanism by promoting an alternative A2 protective phenotype in astrocytes, which could be exploited for development of novel therapeutic strategies for PD and other related chronic neurodegenerative diseases.

Graphical abstract

Correspondence to: Anumantha Kanthasamy; Arthi Kanthasamy.

Conflict of interest:

A.G.K. and V.A. are shareholders of PK Biosciences Corporation (Ames, IA), which is interested in translating mechanistic studies into therapies targeting PK2 signaling. The other authors have no conflicts of interest.

Author Manuscript Author Manuscript Author Manuscript Author Manuscript

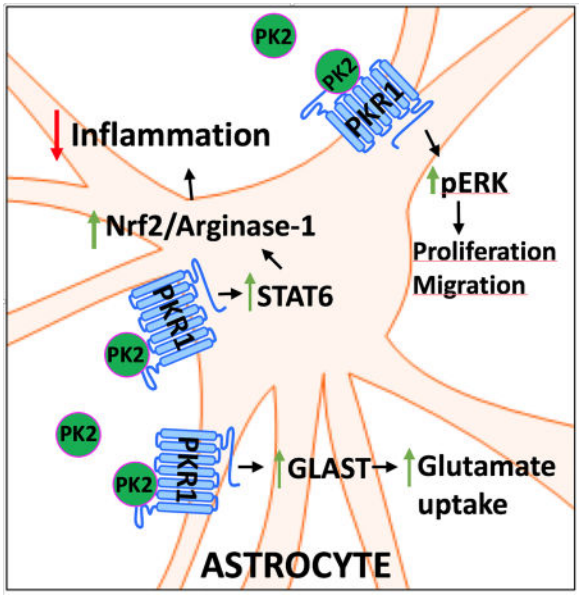

Keywords

PK2; A1 and A2 astrocytes; migration; GFAP; Nrf2; glutamate; inflammation; neuroprotection

Introduction

Astrocytes are key regulators of brain homeostasis and neuronal health. They not only provide metabolic and neurotropic support to neurons but also reduce excitotoxicity via glutamate uptake. Astrocytes can become reactive during neurotoxic stress, commonly referred to as reactive astrogliosis, and some consider this activated state to be a marker for damaged neurons (Ferraguti et al. 2001; Hu et al. 2016). Reactive astrocytes are present in the nigro-striatum of PD patients (Forno et al. 1992; Wakabayashi et al. 1999) as well as in PD animal models (Saura et al. 2003; Teismann et al. 2003; Yasuda et al. 2008). Recent studies have postulated that astrocytes can shift in a stimulus-specific manner towards a harmful, classical pro-inflammatory A1 phenotype or a beneficial, alternate anti-inflammatory A2 phenotype (Jang et al. 2013; Liddelow et al. 2017). This is similar to the classical and alternative phenotype activation states seen in macrophages and microglia (Tang and Le 2016). Although it is known that microglial signaling modulates astrocyte functions (Chen et al. 2015), both the stimulus and the underlying mechanisms leading to astrocyte reactivity and transformation remain elusive. Therefore, ligands that lead to either a classical, pro-inflammatory A1 reactive or alternative, protective A2 reactive state may serve as potential therapeutics for neurodegenerative diseases.

Prokinetcin-2 (PK2) is a small chemokine-like signaling protein that was originally found to potently contract gastrointestinal muscles (Li et al. 2001). It is a mammalian homologue of MIT1, a non-venomous protein in mamba snake venom, and the frog skin protein Bv8 (Ferrara et al. 2004; Schweitz et al. 1999). Subsequently, two G protein-coupled receptors were identified as the prokineticin receptors PKR1 and PKR2 (Lin et al. 2002). Signaling

Author Manuscript Author Manuscript Author Manuscript Author Manuscript

through these receptors is implicated in various physiological functions throughout the body, including hematopoiesis, angiogenesis, reproductive functions, innate immunity and cardiomyocyte protection (Urayama et al. 2007). PK2 also plays a role in circadian rhythms, olfactory bulb biogenesis (Ng et al. 2005; Zhou and Cheng 2005), energy expenditure and homeostasis (Zhou et al. 2012), and neuroprotection (Landucci et al. 2016; Melchiorri et al. 2001).

PK2 expression is generally induced in areas of increased inflammation in the brain and gut (Watson et al. 2012). We recently reported that dopaminergic neurons produce PK2 during early stages of neurotoxic stress as a potential compensatory reaction (Gordon et al. 2016). We demonstrated that soluble PK2 is secreted from dopaminergic neurons treated *in vitro* with TNFα, in multiple *in vivo* mouse models of PD and in human postmortem PD patients (Gordon et al. 2016). We also reported increased levels of PKR2 in the substantia nigra, and importantly that exogenous administration of PK2 protected against MPTP-induced motor-deficits, dopamine depletion and dopaminergic degeneration in animal models of PD. Previous studies also found gene expression in neurons to be higher for PKR2 than for PKR1 (Lin et al. 2002). This pattern contrasts with astrocytes and microglia in the brain where PKR1 gene expression levels exceed those of PKR2 (Zhou 2006). Additionally, PK2 treatment induces cell proliferation and intracellular calcium mobilization in cultured astrocytes. Based on observations of soluble PK2 secreted from damaged dopaminergic neurons, we investigated the role of PK2 signaling in astrocyte reactivity and its functional significance.

Materials and Methods

Reagents

Dulbecco's modified Eagle’s medium (DMEM), MEM media, fetal bovine serum (FBS), L-glutamine, IRDye-tagged secondary antibodies, Hoechst nuclear stain, penicillin, streptomycin, and other cell culture reagents were purchased from Invitrogen (Gaithersburg, MD). Recombinant PK2 was purchased from PeproTech (Rocky Hill, NJ). The primary antibodies for PKR1, PKR2, Nrf2 were ordered from Santa Cruz Biotechnology Inc. (Santa Cruz, CA). GFAP antibody was obtained from Millipore (Billerica, MA). We purchased the phosphorylated STAT6 and native STAT6 antibodies from Cell Signaling (Danvers, MA). The Arginase-1 antibody was ordered from Thermo Fisher (Waltham, MA). The GLAST antibody was generously provided by Dr. Yongjie Yang, Tufts University. Bradford protein assay kit was purchased from Bio-Rad Laboratories (Hercules, CA). Fluo-4 calcium assay and CyQUANT® kits were ordered through Invitrogen.

Animal studies

All animal procedures were approved by Iowa State University’s Institutional Animal Care and Use Committee (IACUC). Eight- to 10-week-old male mice weighing 25–30 g were housed under standard conditions for constant temperature (22 ± 1°C), relative humidity (30%), and a 12-h light cycle with food and water available *ad libitum*. All mice were pre-screened for normal baseline performance during behavioral assessments conducted before

Author Manuscript Author Manuscript Author Manuscript Author Manuscript

randomly assigning animals to experimental groups. Investigators involved with data collection and analysis were not blinded to group allocation.

Stereotaxic injection of rAAV PK2—Stereotaxic surgery was performed exactly as previously described (Gordon et al. 2016). Briefly, C57BL/6NCrl mice (8–10 weeks old) were anesthetized using a ketamine/xylazine mixture. The Angle Two computer-assisted stereotaxic system was used to guide a 10-μl Hamilton syringe needle to the caudate-putamen region of the striatum at the following stereotaxic coordinates in relation to Bregma (mm): −2 ML, 0.5 AP, −4 DV. After advancing the needle through a burr hole drilled in the cranium, 3 μl rAAV-PK2 or rAAV-GFP viral particles (~9×10^{12} total viral particles) were injected into the brain. The animal was allowed to recover for 4 weeks to maximize viral gene expression before euthanization.

Sub-acute MPTP treatment paradigm—Mice received IS20 (10 mg/kg/day) in 50% Miglyol 812N and 50% water mix by oral gavage beginning 1 day before the MPTP treatment, then 5 days of co-treatment with MPTP (20 mg/kg/day, intraperitoneal injection), followed by IS20 treatment daily for another 6 days. Mice were sacrificed 24 h after final treatment. In contrast, control mice received IS20-free 50% Miglyol 812N and 50% water mix, but otherwise were subjected to the same treatment paradigm. Striatum tissues were dissected out and used for gene expression studies.

Cell culture

Primary mouse astrocytes were obtained from the whole brain homogenate of 0- to 3-day-old mouse pups. Astrocytes were collected, isolated and maintained according to a previous method (Gordon et al. 2011) using DMEM media (10% heat-inactive FBS, 100 U/ml penicillin, 100 μg/ml streptomycin, 2 mM glutamate) to grow the cells. Normal human astrocytes (NHA) were obtained from Lonza and grown according to company instructions in astrocyte growth media (AGM, CC-3186) from Lonza. Human U373 astrocytoma cells (ATCC) were grown in MEM media supplemented with 10% FBS, penicillin (100 U/ml) and streptomycin (100 μg/ml), according to ATCC instructions. The NHA and U373 cells were maintained in an incubator at 37°C with 5% CO_2.

CRISPR/Cas9-based knockdown of PKR1 in U373 cells

The lentivirus-based CRISPR/Cas9 knockdown (KD) plasmid, pLV-U6gRNA-Ef1aPuroCas9GFP-PKR1 with the PKR1 gRNA targeting exon 2, was purchased from Sigma-Aldrich. To generate the PKR1 CRISPR lentivirus, the lenti-CRISPR/Cas9 PKR1 KD plasmid and control plasmid were transfected into 293FT cells using the Mission Lentiviral Packaging Mix from Sigma-Aldrich according to the manufacturer's instructions. The lentivirus was harvested 48 h post transfection and titers were measured using the Lenti-X p24 Rapid Titer Kit (Clontech). For stable knockdown of PKR1 in U373 cells, cells were grown in six-well plates with a seeding density of 0.1×10^6 cells per well in growth media, and lentivirus was added to the media at an MOI of 100 and incubated for 24 hr.. After 24 h, fresh media supplemented with puromycin (50 μg/ml) was added to the cells for stable cell selection.

Author Manuscript Author Manuscript Author Manuscript Author Manuscript

Quantitative RT-PCR

Primary mouse astrocytes or human U373 cells were seeded in 75-mm^3 flasks at 2.5×10^6 cells per flask. Treatments were performed in either MEM or DMEM media supplemented with 2% FBS, penicillin (100 U/ml), streptomycin (100 μg/ml), and 2 mM L-glutamine. Cells were treated for 8 h with recombinant PK2 (rPK2, 25 nM) alone or rPK2 cotreated with PC-7 (1 μM). After treatment, cells were collected, pelleted, and resuspended in lysis buffer with β-mercaptoethanol. RNA was isolated using the Absolutely RNA Miniprep kit (Stratagene, San Diego, CA). Reverse transcription was performed using a cDNA synthesis system (Applied Biosystems, Foster City, CA) to convert the RNA into cDNA. Expression levels were determined using real-time PCR with Qiagen RT^2 SYBR Green master mix and validated qPCR mouse primers from Qiagen (Frederick, MD). For normalization of each sample, the mouse gene 18S rRNA (Qiagen Cat. No. PPM57735E) was used as the housekeeping gene. The amount of each template was optimized empirically to maximize efficiency without inhibiting the PCR reaction. According to manufacturer's guidelines, dissociation curves and melting curves were run to ensure that single amplicon peaks were obtained without any non-specific amplicons. The results are reported as fold change in gene expression, which was determined via the $\Delta\Delta C_t$ method using the threshold cycle (C_t) value for the housekeeping gene and for the respective gene of interest in each sample (Livak and Schmittgen 2001).

Western blotting

Astrocytes were collected after treatment, lysed using modified RIPA buffer, homogenized, sonicated, and centrifuged as previously described (Kaul et al. 2005; Kaul et al. 2003). Supernatants were collected, protein concentrations determined and normalized between samples, then stored with loading buffer and DTT. Samples were run on a sodium dodecyl sulfate (SDS) gel electrophoresis. Normalized protein samples were loaded into each well and first separated in a 4% stacking gel and then through a 12–18% resolution gel. Proteins were then transferred to a nitrocellulose membrane. After transfer, the membranes were blocked using Western blocking buffer (Rockland Immunochemicals, Pottstown, PA). Primary antibodies in blocking buffer were then added to the membranes and stored overnight at 4°C. A secondary antibody specific to the primary antibody was added (in either blocking buffer or in 5% low-fat dry milk solution) to the membrane for 1 h. Either β-actin or α-tubulin was used to confirm equal loading into each well of the gels. Densitometric determinations were made using the Odyssey infra-red imaging system (LI-COR, Lincoln, NE).

Immunocytochemistry

For immunocytochemistry (ICC), cells were plated onto coverslips in 24-well plates coated with 0.1% poly-D-Lysine. After cells were treated, 4% paraformaldehyde (PFA) was used to fix the cells for 30 min. The cells were washed with PBS wash buffer. Then blocking buffer containing 2% BSA, 0.2% Triton X-100, and Tween was added to the wells for 1 h. The cells were incubated overnight with primary antibodies in 2% BSA at 4°C. Next, an Alexa Fluor dye-conjugated secondary antibody in 2% BSA was added and incubated at RT on a shaker for 1 h. After washing, Hoechst counterstain was added to the cells for 5–6 min to

Author Manuscript Author Manuscript Author Manuscript Author Manuscript

label nuclei. Coverslips were washed several times then mounted onto slides with Fluoromount mounting media (Molecular probes, Eugene, OR). Cells were imaged under an Eclipse TE2000-U inverted microscope (Nikon, Tokyo, Japan) with a SPOT digital camera (Diagnostic Instruments, Sterling Heights, MI), and all images were processed in MetaMorph 5.7 (Universal Imaging, Downingtown, PA).

For histology, mice were anesthetized using ketamine-xylazine and then perfused with 4% PFA to fix the brain before being extracted and stored in 4% PFA at 4°C. After 48 h, brains were washed with PBS and placed in 30% sucrose for at least 24 h. The brains were then embedded in Optimal Cutting Temperature (OCT) compound and frozen into blocks for sectioning. Brains were sectioned on a cryostat (CryoStar NX70, Thermo Scientific) at −20°C and placed into cryosolution (30% sucrose, 30% ethylene glycol, and 1×PBS). Sections were then washed with PBS and permeabilized with blocking buffer (2% BSA, 0.1% Triton X-100, and Tween) for 1 h at RT. Antibodies directed to the protein of interest were then incubated with the sections overnight at 4°C. After washing with PBS, sections were incubated with Alexa Fluor dye-conjugated secondary antibodies for 1 h at RT. After a final washing with PBS, Hoechst dye (1:5000) was added to the sections for 5 min at RT to stain nuclei. Sections were then mounted on slides using Fluoromount according to the manufacturer's instructions before being visualized and imaged as described above.

GFAP$^+$ cell count and morphological assessment

GFAP diaminobenzedine (DAB) immunostaining was performed as previously described (Ghosh et al. 2012). Briefly, endogenous peroxidases were inhibited, and the sections were blocked with normal goat serum and then incubated overnight with the primary GFAP antibody. Secondary antibody was added for 1 h followed by incubation with ABC solution and finally 2 minutes in DAB substrate. Sections were mounted, air dried, dehydrated before incubation in xylene, and coverslipped.

GFAP$^+$ cell count was determined by using an Eclipse TE2000-U inverted microscope with a SPOT digital camera at 20× magnification. The number of GFAP$^+$ cells was determined by the cell counter plugin for ImageJ. Two fields were counted for each striatum, with three sections per animal and a minimum of 3 animals per group. The numbers were represented as the average number of cells per field of view for each animal.

For GFAP immunostaining density and morphological assessment, 20× and 60× images were taken using an inverted fluorescent microscope (Nikon TE-2000U). Images were imported into ImageJ for morphological analysis. GFAP immunostaining density was measured using the "integrated density" for the 20× image and divided by the number of cells in the field to get the GFAP immunostaining integrated density per cell. Morrison et al demonstrated that the glial processes (Morrison and Filosa 2013) could be analyzed using an ImageJ plugin named Analyze Skeleton (Arganda-Carreras et al. 2010). Briefly, DAB images were converted to binary and then skeletonized in the ImageJ software. The skeletonized image is then fed into the Analyze Skeleton plugin without pruning ends and measuring the long/short branch distance. Detailed information of branch, junction and endpoint number along with branch length metrics is displayed in the results window for the entire image. The results were transferred to an Excel spreadsheet and sorted to only show

Author Manuscript Author Manuscript Author Manuscript Author Manuscript

information with branch numbers between 10 and 300 to remove any non-cellular background. Results were then compared to the number of counted cells in the field to then determine each of the morphology metrics per cell. Three to five fields were used for each section, and then 2–3 biological replicates were used for each experiment. At least 200 cells were measured for each of the morphology assessments. Cell soma size was measured in the same GFAP images in ImageJ by freehand selection outlining each cell soma and then select the “area” analyte to measure. A minimum of 30 cells were analyzed for each treatment in analyzing the soma descriptors, with 2–3 biological replicates for each experiment.

Scratch-wound migration assay

The scratch-wound assay was performed according to Liang et al. (2007). Briefly, astrocytes were grown to a confluent monolayer in 6-well plates. Once the cells were fully confluent, a 1000-μl pipette tip was used to scratch through the cells from top to bottom and from left to right, thereby forming a plus sign to identify similar imaging areas. Cells were triple-washed with serum-free media, treatments were added and wells were imaged for the 0-h timepoint. 10% FBS serum containing media was used as positive control. Endpoint images were taken 24 h after treatment using an inverted fluorescence microscope (Nikon TE-2000U). Measurement of the scratch width was randomly assessed in each group and expressed in microns. This experiment was repeated 3-times using three wells per treatment.

2D Chemotaxis assay

The chemotaxis assay was performed using Ibidi (Planegg, Germany) 2D chemotaxis chambers according to the manufacturer’s guidelines. The U373 astrocytoma cell line was seeded into the middle line of each chamber and allowed to adhere to the plate overnight. The 10% serum-containing DMEM growth media was washed twice with serum-free DMEM media, then either serum-free media or rPK2 was introduced through one of the experimental reservoirs. The cells were imaged at 0 h to ensure that the cells were still attached and then reimaged hourly for 18 h at 10× magnification. Images were taken using an inverted fluorescence microscope (Nikon TE-2000U) and collated using ImageJ software. Cells were tracked to measure migration parameters with the Ibidi Manual Tracking software. A minimum of 50 cells were followed for each treatment to determine overall migration parameters.

Mitochondrial dynamics

To analyze mitochondrial energy dynamics in both primary mouse astrocytes and the U373 human astrocyte cell line, the XFe24 Seahorse analyzer was used to measure OCR and ECAR levels. Astrocytes were plated on Seahorse plates at 80,000 cells/well and allowed to attach overnight in growth media. Cells were then triple-washed with serum-free DMEM media and 500 μl of treatment was added to the wells in serum-free DMEM. After 8 h, the cells were washed twice with and maintained in Seahorse base media supplemented with sodium pyruvate and glutamine. The MitoStress test was performed according to the manufacturer’s guidelines. After testing correct concentrations of the chemicals, 0.75 μM of oligomycin, 1 μM of FCCP, and 0.5 μM rotenone/antimycin were added to the cells to measure mitochondrial dynamics. Analysis was performed through the MitoStress Results Generator available on the Agilent website.

Author Manuscript Author Manuscript Author Manuscript Author Manuscript

Fluo-4 calcium mobilization and CyQUANT proliferation assay

The Fluo-4 NW assay kit was used to test calcium mobilization in primary mouse astrocytes resulting from nanomolar concentrations of rPK2. Cells were plated overnight into 96-well plates in growth media. Cells were then washed with Hank's buffered salt solution (HBSS) and incubated with the Fluo-4 NW dye for one hour. Each plate was then read kinetically using a Synergy-2 multi-mode microplate reader (BioTek, Winooski, VT). After obtaining background readings by reading each plate every 50 ms for 20 sec, rPK2 was injected at the indicated nanomolar concentrations. The net change in fluorescence (Dt), read every 50 ms for 3 min, was obtained after subtracting the background from the maximum signal for each sample.

Astrocyte proliferation was measured using the CyQUANT dye according to manufacturer's guidelines. A standard curve of cell numbers was generated by seeding the astrocytes in a 24-well plate. The same number of astrocytes were seeded in the experimental wells. After 48 h of incubation with treatment of control doses or different doses of rPK2 (5, 10, 25 or 50 nM), 50 μl of CyQUANT dye was added to each well after aspirating medium. After incubation for 30 min at 37°C, fluorescence was measured (excitation 485 nm, emission 538 nm) using the Synergy-2 multi-mode microplate reader. Fluorescence values were compared to the standard curve of cell numbers to generate the treatment-induced cell number.

Glutamate uptake assay

Primary mouse astrocytes were plated into a 24-well plate with 120,000 cells/well in serum-free DMEM media. The media was either untreated (controls) or treated with rPK2 or IS20. After 8 h, the treatment media was washed away with three washes of Krebs-Ringer's buffer. The cells were then incubated with 2 μCi radioactive glutamate for 15 min along with 100 μM L-glutamine in warm Krebs-Ringer's buffer. Media was removed and cells were triple-washed with ice cold Krebs-Ringer's buffer to stop uptake. Next, cells were lysed in 1N NaOH. Radioactivity was measured with a liquid scintillation counter (Tri-Crab 4000, Packard Instrument Co., Fallbrook, California) after the addition of a 5-mL scintillation mixture to each vial. Specific dopamine uptake was expressed as mean counts.

Data analysis

Data analysis was performed using Prism 4.0 (GraphPad Software, San Diego, CA). The data was first analyzed using one-way ANOVA and then Tukey's post-test was performed to compare all treatment groups. Differences of $p \leq 0.05$ were considered statistically significant. Student's t-test was used when comparing two groups.

Results

Receptors for secreted PK2 are expressed on primary mouse and human astrocytes

We recently demonstrated that the chemokine-like protein PK2 is upregulated in cultured dopaminergic neurons and in the substantia nigra of MPTP-treated mice (Gordon et al. 2016). Here, we determined the role of PK2 in astrocytes. First, we examined whether PK2 receptors are present in primary mouse astrocytes. Using qRT-PCR, we found that the PKR1 and PKR2 genes are expressed in both mouse and human primary astrocytes, shown as ΔCt

Author Manuscript Author Manuscript Author Manuscript Author Manuscript

(Figure 1A). However, PKR1 expression levels were 12-fold higher than PKR2 levels in both mouse and human astrocytes when calculated via ΔΔCt. Additionally, we determined PK2 receptor protein levels in ICC (Figure 1B) and confirmed them in Western blot experiments (Figure 1C) in primary mouse astrocytes. The Western blot clearly shows PKR1 protein levels to be higher than PKR2 protein levels measured from the same samples on the same blot, which agrees with our qRT-PCR results (Figure 1A). The fluorescence microscopy images clearly show that PKR1 localizes to the outer cell membrane, whereas PKR2 is localized more towards the cell nucleus. These results are consistent with previously observed results in mouse astrocytes (Koyama et al. 2006).

Since Prokineticin receptors are G protein-coupled receptors, they can be linked to either Gi, Gq or Gs (Zhou 2006). Signaling through Gq induces intracellular calcium mobilization, which could lead to proliferation. Gs increases levels of cAMP, whereas signaling through Gi inhibits the production of cAMP. Therefore, we examined whether recombinant human PK2 (rPK2) could induce functional changes in isolated primary mouse astrocytes, such as increased intracellular calcium and cell proliferation. Astrocyte calcium signaling also has an important function in regulating synaptic strength and could be used as a measure of CNS dysfunction (Álvarez-Ferradas et al. 2015). Using the Fluo4-NW intracellular calcium dye, we demonstrate that rPK2 treatment induced a dose-dependent increase in intracellular calcium in primary mouse astrocytes (Figure 1D). These results demonstrate that rPK2 can elicit a signaling response in these astrocytes through prokineticin receptors. To test whether rPK2 treatment induces cell proliferation, we used CyQUANT dye to measure astrocyte numbers with or without rPK2 treatment. Mouse astrocytes were incubated with 25 nM rPK2 for 48 h. Recombinant PK2 treatment significantly increased cell proliferation when compared to untreated mouse astrocytes (Figure 1E). Taken together, these results suggest that PK2 functions to not only induce intracellular calcium levels by binding to prokineticin receptors but also to increase cell proliferation in primary astrocytes.

Recombinant soluble PK2 induces wound healing in U373 and normal human astrocytes

Since mobilization and induction of intracellular calcium levels are accompanied by astrocyte migration, we utilized a scratch-wound technique to determine if rPK2 induces astrocyte migration. After using a pipette tip to create a “scratch-wound” on a confluent layer of human U373 and normal human astrocytes, we calculated the difference in wound length at 0 h and 24 h after rPK2 treatment to indicate the distance that the cells migrated (Figure 2A). Recombinant PK2 treatment induced a significant increase in wound closure of both the U373 and normal human astrocytes relative to controls (Figure 2B and 2C). As expected, a dramatic increase in wound closure was observed in astrocytes grown in 10% FBS containing media, which was used as a positive control. These results demonstrate that rPK2 treatment induces wound healing in an injured human astrocyte cell line and in normal human astrocytes by promoting migration.

Recombinant human PK2 induces chemotaxis in the U373 human astrocytoma cell line

In the injured or diseased CNS, astrocytes become activated and migrate to the site of injury. Several factors, including TGFβ and bFGF, have demonstrated the ability to cause astrocyte migration (Holland and Varmus 1998; Huang et al. 2012). As a chemokine-like protein, PK2

Author Manuscript Author Manuscript Author Manuscript Author Manuscript

is known to be involved in the activation and migration of several systemic cell types, such as macrophages and monocytes (Ferrara et al. 2004; Martucci et al. 2006). Interestingly, PK2 has demonstrated the ability to activate the ion channel TRPV1 (Vellani et al. 2006), which can increase astrocyte migration (Ho et al. 2014). Given its role in the migration of other cell types, in addition to our discovery that PK2 increases astrocyte wound healing, we examined whether PK2 could be a chemotactic factor for astrocytes. We used the Ibidi 2D chemotaxis slide to test PK2's chemotactic ability in the U373 human astrocytoma cell line. Cells were seeded into a strip in between two media reservoirs on the chemotaxis slide (Figure 3A). One reservoir holds only media, while the other holds the chemotactic factor (rPK2) in media. The slide is designed to allow the chemotactic factor to reach the cells at a concentration curve that is stable for 48 h. If the protein causes chemotaxis in astrocytes, the cells in the middle strip will migrate more towards the chemotactic factor-containing reservoir compared to the media-only reservoir.

The U373 cells were seeded on the slide 10 h before initiating treatment. Images were taken of the seeded cells before and after adding the treatment media to ensure cells were present and appeared healthy. Two experimental migration platforms were used, one with rPK2 in one media reservoir and control in the other. The second platform served as a negative control comparing control media in both reservoirs. Images were taken hourly at 10× magnification for 18 h after the treatment was added to the reservoirs. The images were compiled and stitched together for manual tracking of cells. Images at Hour 0 and 18 for the rPK2 migration platform reveal migration (Figure 3B), which was quantified using the Ibidi manual cell tracking plugin for ImageJ. Beginning at Hour 0, one individual cell was manually selected and tracked at each subsequent timepoint to form a migration track for that cell. This process was repeated to compile migration metrics for over 50 cells for each experimental platform (Figure 3C). Each cell's migration track was analyzed on both 2D axes, with movement toward or away from treatment reservoirs captured on the y-axis, which was oriented perpendicular to the middle line of cells. Lateral movement paralleling both reservoirs was represented on the x-axis. Our analysis of 2D movements produced several migration metrics. The forward migration index on the y-axis (yFMI) indicates the distance traveled by a single cell towards a treatment reservoir, with a larger yFMI indicating a stronger chemotactic effect. The PK2 experimental platform resulted in a significant increase in the yFMI towards the reservoir containing rPK2, whereas the control platform showed no significant yFMI towards either reservoir, as expected (Figure 3D). The x-axis forward migration index (xFMI) showed that neither platform induced an increase in xFMI, or lateral movement in the cell reservoir. Therefore, rPK2 induced a directed migration towards one reservoir resulting from an increased yFMI and little to no change in the xFMI. PK2 also increased migration velocity, or distance travelled each hour (Figure 3E), indicating that cell migration towards the PK2 reservoir was faster than the average control platform cell migration. Similarly, rPK2 treatment increased both the total accumulated distance of the astrocytes and the Euclidean, straight-line distance travelled from the origin (Figure 3F and 3G). Directionality of cell migration can also be gauged by examining the ratio of the Euclidean and accumulated distances, which produces a directionality score close to 1 for straight-line cell migration and less than 1 for non-directional cell migration. Recombinant PK2 treatment significantly increased the directionality score over control

Author Manuscript Author Manuscript Author Manuscript Author Manuscript

treatment (Figure 3H). Collectively, these results demonstrate for the first time that PK2 is a chemotactic factor increasing astrocyte cell migration, similar to what occurs in systemic immune cells.

PK2 shifts mitochondrial metabolism to a more energetic phenotype

Following our demonstration that PK2 can induce mitochondrial biogenesis and help protect mitochondria from stress in neurons (Gordon et al. 2016), we next examined whether PK2 acts on astrocyte mitochondria. Mitochondrial metabolism, oxidative respiration and glycolysis are the drivers underlying shifts in astrocyte cellular responses. Studies have indicated that astrocytes primarily rely on mitochondrial oxidative metabolism for energy production and their mitochondrial dynamics shift in response to pro-inflammatory stimuli or neuronal activity (Hertz et al. 2007; Motori et al. 2013), indicating that mitochondrial dynamics is a useful marker of astrocyte reactivity. Therefore, using the Seahorse XFe24 bioanalyzer, we examined whether PK2 treatment can alter the mitochondrial dynamics of both primary mouse astrocytes (Figure 4A–D) and the U373 human astrocytoma cell line (Figure 4E–H). In primary mouse astrocytes, treatment with rPK2 for 8 h increased the basal oxygen consumption rate (OCR) (Figure 4B) and OCR-mediated ATP production (Figure 4C). We characterized the cell energy phenotype by comparing the rPK2 treatment-induced OCR and the extracellular acidification rate (ECAR). An increasing OCR would indicate a shift in mitochondrial dynamics towards a more aerobic phenotype, whereas an increasing ECAR would indicate a shift towards a more glycolytic phenotype. Interestingly, rPK2 treatment induced increases in both OCR and ECAR levels compared to the control, producing a more energetic phenotype by increasing both energy production pathways in primary mouse astrocytes (Figure 4D). When we conducted the same experiment in the U373 human astrocytoma cell line, we found similar results. Basal OCR (Figure 4F) and ATP production (Figure 4G) were significantly increased with rPK2 treatment compared to the control. The rPK2 treatment also increased ECAR levels in the U373 cell line, which along with the increased OCR, shifted cells toward a more energetic phenotype (Figure 4H). Taken together, these data demonstrate that rPK2, by altering mitochondrial dynamics, can induce an energetic cell phenotype indicative of astrocyte reactivity.

PK2 induces an alternative A2 astrocyte reactive phenotype

Although the specific role for astrocytes in neurodegeneration is still not well-established, studies have demonstrated that reactive astrocytes can either exacerbate inflammation, by producing pro-inflammatory cytokines (Hirsch et al. 2003; Rappold and Tieu 2010), or help protect against inflammation through anti-oxidant response elements such as Nrf2 and reduced glutathione (Dias et al. 2013; Vargas et al. 2008). Similar to classical, pro-inflammatory M1- and alternate, anti-inflammatory M2-like microglial phenotypes, the different phenotypes of reactive astrocytes can likewise be categorized as classical A1 and alternate A2 (Jang et al. 2013; Liddelow et al. 2017). Reactive A1 astrocytes leads to an increase in the release of factors that are destructive to synapses, whereas reactivity of A2 astrocytes results in release of neurotrophic factors and other protective molecules that are beneficial to neurons. Knowing that PK2 can activate astrocytes, we investigated whether PK2-induced astrocyte reactivity leads to either an A1 or A2 phenotype. We first determined whether rPK2 treatment shifts astrocyte reactivity towards an A1 phenotype favoring

Author Manuscript Author Manuscript Author Manuscript Author Manuscript

increased production and release of pro-inflammatory cytokines. Primary mouse astrocytes were treated with rPK2 for 8 h and prepared for qPCR analysis of pro-inflammatory cytokines or treated for 12 h to determine secreted pro-inflammatory protein levels. Gene expression analysis with rPK2 treatment showed no change in the expression of the inflammatory cytokines IL-1β and TNFα (Figure 5A). Conditioned media from the 12-h treatment was examined using a multiplex bead assay on the Bio-Plex 200 for the pro-inflammatory cytokines IL-1β, IL-6, and TNFα. The rPK2-conditioned media significantly reduced the basal protein levels of all three pro-inflammatory cytokines (Figure 5B). These results indicate that although PK2 appears to cause astrocyte reactivity based on morphology, it does not increase the production or release of pro-inflammatory cytokines but instead reduces their basal levels.

Next, we determined whether rPK2 could induce an A2 reactive phenotype by measuring anti-oxidant or anti-inflammatory response factors in primary mouse astrocytes. Arginase-1 and inducible nitric oxide synthase (iNOS) are enzymes that compete for l-arginine. This allows arginase-1 to modulate the amount of nitric oxide (NO) produced by iNOS. Therefore, the ratio of arginase-1 to iNOS gene expression and protein level is an important indicator of the astrocytes' inflammatory status, with a higher ratio of arginase-1 indicating an anti-inflammatory response, while a pro-inflammatory response is indicated by higher iNOS expression. Previous studies have found astrocytes produce more arginase-1 during stressful conditions, such as a stroke (Quirié et al. 2013). Using qPCR, we determined that rPK2 treatment significantly increased arginase-1 gene expression, while iNOS gene expression was significantly decreased (Figure 5C). These effects of rPK2 treatment were completely attenuated with co-treatment of the prokineticin receptor antagonist PC-7. Similarly, the rPK2-induced decrease in iNOS gene expression was confirmed by decreased iNOS staining in ICC experiments on primary mouse astrocytes (Figure 5D).

Overexpression of Nrf2 in astrocytes was recently shown to protect dopaminergic neurons from neurotoxicity (Gan et al. 2012). Here, we found that rPK2 treatment significantly increased the mRNA expression of both Nrf2 and a target gene of Nrf2, Prdx2, (Figure 5E) as well as Nrf2 protein level by ICC (Figure 5F) and Western blot (Figure 5G) in mouse primary astrocytes. Co-treatment with PC-7 attenuated the rPK2-induced increase in Nrf2 protein level (Figure 5F and 5G). These results indicate that exogenously added rPK2 can stimulate astrocytes to induce expression of anti-oxidant and anti-inflammatory factors such as arginase-1 and Nrf2.

Lenti-PK2 overexpression induces the anti-oxidant response proteins arginase-1 and Nrf2

Next, we used a lentiviral delivery system to overexpress GFP-tagged PK2 or GFP-alone in primary mouse astrocytes (Figure 6A). Gene expression analysis revealed that PK2 overexpression increased both arginase-1 and Nrf2, while iNOS gene expression was not altered (Figure 6B). Examining the conditioned media of primary mouse astrocytes overexpressing PK2 revealed no change in the basal secretion of the pro-inflammatory cytokines IL-1β, IL-6, TNFα when compared to GFP controls (Figure 6C). However, densitometric analyses of the Western blot revealed that Nrf2 protein level was significantly

Author Manuscript Author Manuscript Author Manuscript Author Manuscript

increased in PK2-GFP-overexpressing astrocytes but not in GFP-overexpressing astrocytes (Figure 6D), similar to that observed with rPK2 treatment.

Since STAT6 phosphorylation has been implicated in alternative activation of microglia and macrophages (Hu et al. 2015), we measured STAT6 phosphorylation in PK2-induced astrocyte reactivity. PK2 overexpression significantly increased phosphorylated STAT6 protein level compared to GFP overexpression, whereas total STAT6 protein level was not altered (Figure 6D). Taken together, these results demonstrate that rPK2 administration or PK2 overexpression shifts astrocytes toward an A2 reactive phenotype via STAT6 signaling to produce more anti-oxidant proteins such as arginase-1 and Nrf2.

PK2 overexpression induces GFAP upregulation and increases astrocyte numbers and soma size

Astrocyte morphology is a dynamic phenomenon that can have significant impact on neuronal synapses, and therefore represents an important measure of astrocyte reactivity (Heller and Rusakov 2015). Under basal conditions, astrocytes are characterized by thin cell bodies, elongated processes, and they express low levels of glial fibrillary acidic protein (GFAP). Upon reactivity, the cell soma and primary processes undergo hypertrophy, and astrocytes express higher levels of GFAP (Pekny and Pekna 2014). Previously, PK2 was found to activate immune cells and modulate systemic inflammation (Monnier and Samson 2008). Therefore, we stereotaxically injected GFP-tagged PK2 housed in an AAV 2/5 viral delivery system under the power of the CMV promoter directly into the mouse striatum. Controls were injected with AAV2/5-GFP or saline. Four weeks post-injection, GFP-tagged PK2 expression was widespread in the striatum as seen by fluorescence microscopy (Figure 7A). This was accompanied by a significant increase in GFAP expression in the striatum of AAV-PK2-GFP injected animals (Figure 7A and 7B) compared to mice only injected with AAV-GFP.

To further determine whether PK2 overexpression results in altered astrocyte morphology, we performed DAB immunostaining for GFAP on striatal sections from either AAV-GFP or AAV-PK2-GFP injected animals. Control striata contained cells with characteristics resembling resting astrocytes with thin cell bodies, elongated processes, low GFAP expression and fewer GFAP-positive cells (Figure 7C). Consistent with the Western blotting results, AAV-PK2-GFP injections increased the number of GFAP-positive cells in the striatum. These GFAP-positive cells exhibited cell soma hypertrophy, obvious hypertrophy of the primary processes, and an increased amount of GFAP protein immunostaining (Figure 7C). In contrast, AAV-GFP alone did not significantly increase any of these characteristics. Quantification of the DAB immunostain revealed that AAV-PK2-GFP induced a significant increase in the number of GFAP-positive cells (Figure 7D), amount of GFAP protein per cell (Figure 7E), and the cell soma size (Figure 7F). Taken together, these results demonstrate that PK2 overexpression induced significant morphological changes in GFAP-positive cells that are indicative of astrocyte reactivity.

Author Manuscript Author Manuscript Author Manuscript Author Manuscript

PK2 overexpression reduces total number of astrocyte processes and endpoints and promotes alternative reactivity *in vivo*

Another indication of astrocyte reactivity is the retraction of cytoplasmic processes (Kang et al. 2014). Since rPK2 could induce astrocyte migration in culture, retraction of processes and endpoints in astrocytes *in vivo* could be because those cells are currently migrating or preparing for migration. Using an ImageJ plugin developed to measure branching (Morrison and Filosa 2013), we analyzed astrocyte processes following overexpression of PK2. GFAP DAB immunostaining images were uploaded into ImageJ (Figure 8A), converted into binary images, and finally reduced to a skeleton image (Figure 8B) that was then analyzed to show every branch (orange), junction (purple) and endpoint (blue) (Figure 8C). This analysis allowed us to determine the length of processes and the number of branches, junctions and process endpoints. AAV-PK2-GFP significantly reduced the number of astrocyte processes when compared to PBS control injection, whereas AAV-GFP did not result in a significant reduction (Figure 8D). Also, the number of astrocytic process endpoints per cell was significantly reduced following AAV-PK2-GFP injection (Figure 8E) compared to AAV-GFP or PBS control. Recently, Liddelow *et al.* (2017) published a panel of genes which are differentially expressed in A1 and A2 alternatively activated astrocytes. In their panel, Serping 1 is upregulated in A1 phenotype and S100a10, PTX3, SPHK1 and TN4SF1 are upregulated in A2 phenotype. We did not observe any change in mRNA levels of Serping 1 in AAV-PK2-treated compared to AAV-GFP-treated astrocytes (Figure 8F). On the other hand, we observed significantly increased mRNA levels of PTX3, SPHK1 and TM4SF1, but only modestly increased S100a10 mRNA levels (Figure 8F), in AAV-PK2-treated compared to AAV-GFP-treated astrocytes. Taken together, these results quantitatively demonstrate that PK2 overexpression can increase astrocyte reactivity *in vivo* and induce expression of genes associated with an alternatively reactive A2 phenotype.

PKR1 agonist promotes alternative astrocyte reactivity in in cell culture and MPTP animal models of PD

Recently, Gasser *et al.* (2015) screened a library of PKR1 non-peptide agonist compounds for protecting cardiomyocytes. One of their compounds, IS20, activated the downstream prokineticin receptor signaling pathways, such as Akt and ERK, and protected cardiomyocytes against myocardial infarction (Gasser et al. 2015). Since astrocytes mainly express PKR1, we determined if IS20 was capable of activating astrocytes in a similar manner to rPK2 and PK2 overexpression. Treatment with IS20 (10 μM) significantly increased mitochondrial respiration and ATP production (Figure 9A) in primary mouse astrocytes, suggesting a shift in the cellular energy phenotype towards a more energetic role compared to control treatment. These results indicate that IS20 can activate astrocytes in a similar manner to rPK2 treatment. Next, we found that mRNA levels of anti-oxidant genes, such as arginase-1 and Nrf2, were also significantly increased, whereas iNOS gene expression was decreased compared to the control (Figure 9B). We validated the gene expression results by examining the protein level of these key reactivity proteins using Western blotting techniques. In concordance with our qPCR results, GFAP, arginase-1 and Nrf2 significantly increased compared to control (Figure 9C). Similar to AAV-PK2 expression and rPK2 treatment, IS20 (10 μM) did not alter mRNA expression levels of Serping 1, whereas IS20 30 μM led to a significant decrease in gene expression of this gene

Author Manuscript Author Manuscript Author Manuscript Author Manuscript

associated with the A1 phenotype (Figure 9D). However, 10 μM IS20 induced increases in PTX3 mRNA levels (Figure 9E) compared to control treatments. To further corroborate these findings, we examined the effects of genetic knockdown of PKR1 on A1/2 marker gene expression in the U373 cells. Transduction of U373 cells with the CRISPR/Cas9-based PKR1 knockdown (KD) lentivirus almost completely abolished PKR1 mRNA expression (Figure 9F, left panel). As shown in Figure 9F right panel, CRISPR/Cas9-based PKR1 knockdown dramatically inhibited IS20-induced mRNA upregulation of the anti-oxidant factors arginase-1 and Nrf2, whereas iNOS mRNA expression was not affected. Taken together, these results demonstrate that IS20, a non-peptide PKR1 agonist, can activate astrocytes and upregulate both the mRNA and protein expression of the anti-oxidant factors arginase-1 and Nrf2 as well as the PTX3 mRNA level, which is associated with the A2 reactive phenotype.

In a classic animal model of Parkinsonism, sub-acute MPTP administration (Figure 9G) significantly increased mRNA levels of the proinflammatory A1 gene GBP2 (Figure 9H), whereas IS20 co-treatment inhibited MPTP-induced increases in GBP2 mRNA levels, suggesting IS20 may be capable of protecting against MPTP-induced astrocyte A1 reactive phenotype (Figure 9H). On the other hand, MPTP-treatment alone induced a statistically significant decrease in mRNA levels of the SPHK1 and SLC10a6 genes (Figure 9I). Co-treatment with IS20 protected against MPTP-induced decreases in SPHK1 and SLC10a6 mRNA levels, suggesting IS20 can protect against MPTP-induced suppression of the A2 phenotype (Figure 9I). Taken together, these results demonstrate that MPTP-induced increases in the A1 phenotype gene GBP2 and decreases in A2 phenotype SPHK1 and SLC10a6 genes were suppressed by the non-peptide PKR1 agonist IS20.

Recombinant PK2 and IS20 treatments increased glutamate uptake via GLAST upregulation

Astrocytes are known to help protect neurons through multiple mechanisms, with one of those being the uptake of glutamate to prevent excitotoxicity (Sattler and Rothstein 2006). Astrocyte uptake of glutamate reduces the extracellular levels but can also induce astrocyte reactivity and alter multiple astrocyte functions (Morales and Rodriguez 2012), so it is important to examine astrocyte-mediated glutamate uptake. Interestingly, pro-inflammatory cytokines, such as TNFα, decrease the expression of glutamate transporters, especially GLAST (Dumont et al. 2014). Therefore, we used radiolabeled glutamate to determine whether rPK2 treatment could increase glutamate uptake by primary mouse astrocytes. Treating primary mouse astrocytes with rPK2 or the PKR1 chemical agonist IS20 for 8 h, along with IL-4 as a positive control, led to increased glutamate uptake compared to control cells (Figure 10A). Although astrocytes that are cultured without the presence of neurons express low levels of GLT-1, GLAST is expressed at normal levels (Swanson et al. 1997). We first confirmed that the primary mouse astrocytes did not express GLT-1 with undetectable gene expression levels in control or treated cells (unpublished). Interestingly, we found that rPK2 treatment increased GLAST gene expression (Figure 10B) and protein level (Figure 10C) in primary mouse astrocytes, similar to that observed with the positive control IL-4. Taken together, these data indicate that PK2 signaling can lead to functional

Author Manuscript Author Manuscript Author Manuscript Author Manuscript

changes in astrocytes that reduce extracellular glutamate through upregulation of the glutamate transporter GLAST, thereby potentially protecting neurons from excitotoxicity.

Discussion

Astrocytes become reactive during the neurodegenerative process. Although the mechanisms underlying reactive astrogliosis are unclear, until recently it was viewed as a defensive reaction counteracting acute stress, restoring CNS homeostasis and limiting tissue damage. Considerable evidence now shows that reactive astrocytes can shift to either a predominantly harmful or protective reactive state. Since astrocytes respond to multiple stimuli, it is possible that the harmful or beneficial effects of reactive astrocytes will be stimulus- or disease-specific (Jang et al. 2013; Liddelow et al. 2017). Pro-inflammatory cytokines such as TNFα and IL-1β stimulate astrocytes toward a predominantly harmful reactive state, whereas stimulation with the anti-inflammatory cytokine IL-4 can lead to a more protective or restorative reactive state (Jang et al. 2013). These different reactive states have been termed A1, for the classical, pro-inflammatory state, and A2, for the protective, restorative state (Liddelow et al. 2017). Activated microglia can lead to A1 reactive astrocytes, which become cytotoxic and induce neurodegeneration. The A1/A2 terminology was derived from the similar M1 and M2 activation states found in macrophages and microglia. A1 astrocyte reactivity is evident in a wide range of neurodegenerative diseases, including PD, Alzheimer's disease, Huntington's disease, amyotrophic lateral sclerosis and multiple sclerosis. On the other hand, A2 astrocytes can resolve inflammation and protect neurons and have primarily been found in ischemic injury, potentially resolving the inflammatory response (Liddelow et al. 2017). It is therefore important to examine these reactive states and understand the mechanisms behind both A1 and A2 reactivity. Zamanian *et al.* (2012) found that over 50% of altered astrocyte gene expression differed between an ischemic injury model and an LPS inflammatory response model. Therefore, it is important to understand neuron-astrocyte signaling in pathological conditions such as PD. Recently, we demonstrated that dopaminergic neurons produce and secrete high levels of the chemokine-like signaling protein PK2, as evidenced in animal models of PD as well as in post-mortem tissues from human PD patients (Gordon et al. 2016). In the present study, we demonstrate that both types of prokineticin receptors are expressed by primary mouse and human astrocytes. PKR1 is expressed over 12-fold higher than PKR2 and is mainly colocalized to the outer cell plasma membrane. Similar to Koyama *et al.* (2006), our *in vitro* treatments with human rPK2 increased intracellular calcium and cell proliferation in a primary astrocyte culture (Figure 1).

For the first time, we demonstrate that treatment with rPK2 increased astrocyte wound healing, chemotaxis, and shifted mitochondrial metabolism to a more energetic phenotype in both primary mouse astrocytes as well as in a human astrocyte cell line (U373). Also for the first time, we show that rPK2 treatment or PK2 overexpression reduced the expression of the pro-inflammatory factors IL-1β, IL-6, TNFα and iNOS, and increased the expression of the anti-oxidant genes arginase-1 and Nrf2. Together, these are the first results demonstrating that a protein produced by neurons can increase cultured human astrocyte migration and shift primary mouse astrocytes to an anti-inflammatory A2 reactive phenotype. Although astrocyte reactivity has been used routinely as a marker for neurodegeneration and

Author Manuscript Author Manuscript Author Manuscript Author Manuscript

neuroinflammation, the consequences of this reactivity remain unclear. We demonstrate that PK2 can induce astrocyte reactivity both *in vitro*, by analyzing mitochondrial dynamics, and *in vivo* in the mouse striatum as evidenced by the AAV-PK2-induced increase in the number of GFAP-positive cells, the amount of GFAP immunostaining per cell, and the increased soma size of astrocytes. Similarly, analysis of astrocyte cellular branch patterns revealed reduced number of astrocyte branches and endpoints compared to AAV-GFP overexpression. Previously, we found that damaged dopaminergic neurons of the substantia nigra produce higher levels of PK2 (Gordon et al. 2016), which when taken together with the results here indicates that PK2 overexpression in the mouse striatum can activate astrocytes and induce their migration toward damaged dopaminergic neurons. Our observation of increased migration and proliferation following PK2 treatment-induced astrocyte reactivity is consistent with the increased number of reactive astrocytes seen in the nigro-striatal pathway in animal models of PD and in PD patients (Hamby and Sofroniew 2010; Miklossy et al. 2006). Thus, an increase in PK2 production and secretion from dopaminergic neurons can induce astrocytes to migrate to damaged neurons to provide anti-oxidant support. Collectively, these results demonstrate that PK2 secreted from damaged neurons likely signals to astrocytes, causing them to migrate to the site of injury and transform them to the beneficial A2 phenotype.

Measurements of mitochondrial dynamics are useful indicators of cell health and metabolism. Reduction of mitochondrial oxidative respiration through fragmentation of the mitochondrial network in neurons is an indicator of cell stress as found in pathological conditions like PD. This can develop from genetic defects in proteins such as PINK1 and Parkin, or through environmental factors that disrupt the mitochondrial electron transport chain (Lim et al. 2012; Van Laar and Berman 2013). Similarly, mitochondrial dynamics of glial cells can serve as an indicator of the inflammatory reactive state, including regulation of the astrocyte response to injury (Jackson and Robinson 2017). Microglia treated with the purified endotoxin lipopolysaccharide (LPS) exhibit reduced basal and peak oxidative respiration rates (Orihuela et al. 2016). Under basal conditions, astrocytes rely on glycolysis for energy production, but they switch to higher oxidative respiration once activated by certain stimuli (Hertz et al. 2007). Inflammation from an acute brain injury was found to increase mitochondrial fragmentation in astrocytes and impair mitochondrial bioenergetics, while increasing the production of ROS (Motori et al. 2013). Recombinant PK2 treatment of cultured primary mouse astrocytes or the U373 human astrocyte cell line increased the basal levels of oxidative respiration along with glycolysis (Figure 4). The rPK2-induced increase in basal respiration of astrocytes is consistent with our previous findings where rPK2 increased mitochondrial biogenesis in neurons (Gordon et al. 2016). However, it is more likely that reactive astrocytes require more energy for proliferation and migration, similar to previous reports for mitochondrial dynamics in microglia (Jiang and Cadenas 2014; Orihuela et al. 2016). Collectively, rPK2 treatment increased overall ATP production and basal respiration of cultured astrocytes, which indicates a possible alternative A2 reactive state of these cells due to inflammatory stimuli inducing the opposite effect.

Oxidative stress and excitotoxicity have been implicated in the progression of PD, with increased extracellular glutamate and ROS inducing dopaminergic neurodegeneration (Ambrosi et al. 2014; Hwang 2013). Although astrocytes were traditionally viewed as

Author Manuscript Author Manuscript Author Manuscript Author Manuscript

support cells for the neurons of the CNS, evidence indicates that astrocytes can contribute to inflammatory damage of the CNS (Colombo and Farina 2016; Liddelow et al. 2017). Others report that overexpression of Nrf2 in astrocytes can protect dopaminergic neurons from cell death (Gan et al. 2012). Stimulating the increased production of such antioxidant proteins in astrocytes could be a promising therapeutic avenue. Although the mechanisms behind Nrf2 induction in astrocytes are still being elucidated, communication from activated microglia is clearly involved (Correa et al. 2011). Importantly, PK2 signaling in astrocytes does not increase inflammatory factors such as pro-inflammatory cytokines or iNOS. On the other hand, PK2 can increase protective factors such as the anti-oxidant proteins arginase-1, Mrc1, Prdx2 and, most importantly, Nrf2 at both the genetic and protein levels associated with the astrocytes A2 reactive phenotype. AAV-PK2 also induced increases in S100a10, PTX3, SPHK1 and TM4SF1 gene expression associated with induction of the anti-inflammatory A2 reactive phenotype. Interestingly, the non-peptide PKR1 agonist IS20 activated cultured astrocytes and increased both arginase-1 and Nrf2 protein levels. Since this response occurs without elevating pro-inflammatory cytokines, then PK2-induced reactive astrocytes could lead to a more neuroprotective phenotype. Utilizing a CRISPR/Cas9 lentiviral knockdown technique, we found that almost completely knocking down PKR1 completely abolished the IS20-mediated increase in the anti-inflammatory mediators arginase-1 and Nrf2, while not affecting iNOS gene expression (Figure 9F). Therefore, the PK2-mediated signaling in astrocytes is mainly mediated by signaling through the PKR1 receptor. When we administered MPTP in a classical animal model of PD, IS20 co-treatment restored mRNA levels of the A2-phenotype genes SPHK1 and SCL10a6, which were otherwise severely reduced in animals treated with MPTP alone. Similarly, IS20 blocked MPTP-induced increases of GBP2 mRNA levels associated with the proinflammatory A1-phenotype. Furthermore, prokineticin signaling increases glutamate uptake by increasing the gene expression and protein level of GLAST in cultured astrocytes and could offer neuroprotection from excitotoxicity. Scavenging of glutamate by astrocytes is a key mechanism of neuroprotection, and increasing their ability to remove glutamate has been demonstrated to protect dopaminergic neurons (Yao et al. 2005). Interestingly, Voloboueva *et al.* (2007) reported that mitochondrial impairment of astrocytes reduces their ability to uptake glutamate, resulting in exaggerated neuronal cell death in a co-culture system. Similarly, Hu *et al.* (2000) had shown that inflammatory cytokine treatment decreased glutamate uptake in cultured human fetal astrocytes. Ours is the first report of the cytokine-like signaling protein PK2 inducing anti-oxidant factors along with increased glutamate uptake in cultured astrocytes.

Previously, we demonstrated that dopaminergic neurons produced and secreted PK2 (Gordon et al. 2016), which directly protected dopaminergic neurons through activation of the ERK and AKT pathways. In this study, we report for the first time that PK2 signaling can induce alternative A2 reactivity of astrocytes, stimulate astrocyte migration, induce the production of neuroprotective factors such as Nrf2, and increase glutamate uptake. These effects are mainly mediated via PKR1 signaling, with a PKR1 chemical agonist increasing the A2 phenotype and CRISPR/Cas9 PKR1 knockdown abolished this increase. This opens the opportunity for exploiting prokineticin signaling to protect dopaminergic neurons in PD through alternative A2 astrocyte reactivity and increased anti-oxidant support. Further

Author Manuscript Author Manuscript Author Manuscript Author Manuscript

exploration of PK2 signaling in neuron-glia crosstalk could be an important avenue for developing novel therapeutic approaches to treating neurodegenerative diseases.

Acknowledgments

This study was supported by NIH R01 grants NS078247, NS088206 and ES026892. The W. Eugene and Linda Lloyd Endowed Chair to AGK and the Dean Endowed Professorship to AK are also acknowledged. We also thank Mr. Gary Zenitsky for assistance in preparing this manuscript.

References

Álvarez-Ferradas C, Morales JC, Wellmann M, Nualart F, Roncagliolo M, Fuenzalida M, Bonansco C. Enhanced astroglial Ca2+ signaling increases excitatory synaptic strength in the epileptic brain. Glia. 2015; 63:1507–21. [PubMed: 25980474]

Ambrosi G, Cerri S, Blandini F. A further update on the role of excitotoxicity in the pathogenesis of Parkinson's disease. J Neural Transm (Vienna). 2014; 121:849–59. [PubMed: 24380931]

Arganda-Carreras I, Fernández-González R, Muñoz-Barrutia A, Ortiz-De-Solorzano C. 3D reconstruction of histological sections: Application to mammary gland tissue. Microsc Res Tech. 2010; 73:1019–29. [PubMed: 20232465]

Chen SH, Oyarzabal EA, Sung YF, Chu CH, Wang Q, Chen SL, Lu RB, Hong JS. Microglial regulation of immunological and neuroprotective functions of astroglia. Glia. 2015; 63:118–31. [PubMed: 25130274]

Colombo E, Farina C. Astrocytes: Key Regulators of Neuroinflammation. Trends Immunol. 2016; 37:608–20. [PubMed: 27443914]

Correa F, Ljunggren E, Mallard C, Nilsson M, Weber SG, Sandberg M. The Nrf2-inducible antioxidant defense in astrocytes can be both up- and down-regulated by activated microglia:Involvement of p38 MAPK. Glia. 2011; 59:785–99. [PubMed: 21351160]

Dias V, Junn E, Mouradian MM. The Role of Oxidative Stress in Parkinson's Disease. Journal of Parkinson's disease. 2013; 3:461–491.

Dumont AO, Goursaud S, Desmet N, Hermans E. Differential regulation of glutamate transporter subtypes by pro-inflammatory cytokine TNF-alpha in cortical astrocytes from a rat model of amyotrophic lateral sclerosis. PLoS One. 2014; 9:e97649. [PubMed: 24836816]

Ferraguti F, Corti C, Valerio E, Mion S, Xuereb J. Activated astrocytes in areas of kainate-induced neuronal injury upregulate the expression of the metabotropic glutamate receptors 2/3 and 5. Exp Brain Res. 2001; 137:1–11. [PubMed: 11310162]

Ferrara N, LeCouter J, Lin R, Peale F. EG-VEGF and Bv8: a novel family of tissue-restricted angiogenic factors. Biochim Biophys Acta. 2004; 1654:69–78. [PubMed: 14984768]

Forno LS, DeLanney LE, Irwin I, Di Monte D, Langston JW. Astrocytes and Parkinson's disease. Prog Brain Res. 1992; 94:429–36. [PubMed: 1287728]

Gan L, Vargas MR, Johnson DA, Johnson JA. Astrocyte-specific overexpression of Nrf2 delays motor pathology and synuclein aggregation throughout the CNS in the alpha-synuclein mutant (A53T) mouse model. J Neurosci. 2012; 32:17775–87. [PubMed: 23223297]

Gasser A, Brogi S, Urayama K, Nishi T, Kurose H, Tafi A, Ribeiro N, Desaubry L, Nebigil CG. Discovery and cardioprotective effects of the first non-Peptide agonists of the G protein-coupled prokineticin receptor-1. PLoS One. 2015; 10:e0121027. [PubMed: 25831128]

Ghosh A, Kanthasamy A, Joseph J, Anantharam V, Srivastava P, Dranka BP, Kalyanaraman B, Kanthasamy AG. Anti-inflammatory and neuroprotective effects of an orally active apocynin derivative in pre-clinical models of Parkinson's disease. J Neuroinflammation. 2012; 9:241. [PubMed: 23092448]

Gordon R, Hogan CE, Neal ML, Anantharam V, Kanthasamy AG, Kanthasamy A. A simple magnetic separation method for high-yield isolation of pure primary microglia. J Neurosci Methods. 2011; 194:287–96. [PubMed: 21074565]

Gordon R, Neal ML, Luo J, Langley MR, Harischandra DS, Panicker N, Charli A, Jin H, Anantharam V, Woodruff TM, et al. Prokineticin-2 upregulation during neuronal injury mediates a

Author Manuscript Author Manuscript Author Manuscript Author Manuscript

compensatory protective response against dopaminergic neuronal degeneration. Nat Commun. 2016; 7:12932. [PubMed: 27703142]

Hamby ME, Sofroniew MV. Reactive astrocytes as therapeutic targets for CNS disorders. Neurotherapeutics. 2010; 7:494–506. [PubMed: 20880511]

Heller JP, Rusakov DA. Morphological plasticity of astroglia: Understanding synaptic microenvironment. Glia. 2015; 63:2133–51. [PubMed: 25782611]

Hertz L, Peng L, Dienel GA. Energy metabolism in astrocytes: high rate of oxidative metabolism and spatiotemporal dependence on glycolysis/glycogenolysis. J Cereb Blood Flow Metab. 2007; 27:219–49. [PubMed: 16835632]

Hirsch EC, Breidert T, Rousselet E, Hunot S, Hartmann A, Michel PP. The role of glial reaction and inflammation in Parkinson's disease. Ann N Y Acad Sci. 2003; 991:214–28. [PubMed: 12846989]

Ho KW, Lambert WS, Calkins DJ. Activation of the TRPV1 cation channel contributes to stress-induced astrocyte migration. Glia. 2014; 62:1435–51. [PubMed: 24838827]

Holland EC, Varmus HE. Basic fibroblast growth factor induces cell migration and proliferation after glia-specific gene transfer in mice. Proc Natl Acad Sci U S A. 1998; 95:1218–23. [PubMed: 9448312]

Hu S, Sheng WS, Ehrlich LC, Peterson PK, Chao CC. Cytokine effects on glutamate uptake by human astrocytes. Neuroimmunomodulation. 2000; 7:153–9. [PubMed: 10754403]

Hu X, Leak RK, Shi Y, Suenaga J, Gao Y, Zheng P, Chen J. Microglial and macrophage polarization—new prospects for brain repair. Nat Rev Neurol. 2015; 11:56–64. [PubMed: 25385337]

Hu X, Yuan Y, Wang D, Su Z. Heterogeneous astrocytes: Active players in CNS. Brain Res Bull. 2016; 125:1–18. [PubMed: 27021168]

Huang C, Wu J, Liao R, Zhang W. SKF83959, an agonist of phosphatidylinositol-linked D(1)-like receptors, promotes ERK1/2 activation and cell migration in cultured rat astrocytes. PLoS One. 2012; 7:e49954. [PubMed: 23185493]

Hwang O. Role of oxidative stress in Parkinson's disease. Exp Neurobiol. 2013; 22:11–7. [PubMed: 23585717]

Jackson JG, Robinson MB. Regulation of mitochondrial dynamics in astrocytes: Mechanisms, consequences, and unknowns. Glia. 2017

Jang E, Kim JH, Lee S, Kim JH, Seo JW, Jin M, Lee MG, Jang IS, Lee WH, Suk K. Phenotypic polarization of activated astrocytes: the critical role of lipocalin-2 in the classical inflammatory activation of astrocytes. J Immunol. 2013; 191:5204–19. [PubMed: 24089194]

Jiang T, Cadenas E. Astrocytic metabolic and inflammatory changes as a function of age. Aging Cell. 2014; 13:1059–1067. [PubMed: 25233945]

Kang K, Lee SW, Han JE, Choi JW, Song MR. The complex morphology of reactive astrocytes controlled by fibroblast growth factor signaling. Glia. 2014; 62:1328–44. [PubMed: 24796693]

Kaul S, Anantharam V, Kanthasamy A, Kanthasamy AG. Wild-type alpha-synuclein interacts with pro-apoptotic proteins PKCdelta and BAD to protect dopaminergic neuronal cells against MPP+-induced apoptotic cell death. Brain Res Mol Brain Res. 2005; 139:137–52. [PubMed: 15978696]

Kaul S, Kanthasamy A, Kitazawa M, Anantharam V, Kanthasamy AG. Caspase-3 dependent proteolytic activation of protein kinase C delta mediates and regulates 1-methyl-4-phenylpyridinium (MPP+)-induced apoptotic cell death in dopaminergic cells: relevance to oxidative stress in dopaminergic degeneration. Eur J Neurosci. 2003; 18:1387–401. [PubMed: 14511319]

Koyama Y, Kiyo-oka M, Osakada M, Horiguchi N, Shintani N, Ago Y, Kakuda M, Baba A, Matsuda T. Expression of prokineticin receptors in mouse cultured astrocytes and involvement in cell proliferation. Brain Res. 2006; 1112:65–9. [PubMed: 16901473]

Landucci E, Lattanzi R, Gerace E, Scartabelli T, Balboni G, Negri L, Pellegrini-Giampietro DE. Prokineticins are neuroprotective in models of cerebral ischemia and ischemic tolerance in vitro. Neuropharmacology. 2016; 108:39–48. [PubMed: 27140692]

Li M, Bullock CM, Knauer DJ, Ehlert FJ, Zhou QY. Identification of two prokineticin cDNAs: recombinant proteins potently contract gastrointestinal smooth muscle. Mol Pharmacol. 2001; 59:692–8. [PubMed: 11259612]

Author Manuscript Author Manuscript Author Manuscript Author Manuscript

Liang CC, Park AY, Guan JL. In vitro scratch assay: a convenient and inexpensive method for analysis of cell migration in vitro. Nat Protoc. 2007; 2:329–33. [PubMed: 17406593]

Liddelow SA, Guttenplan KA, Clarke LE, Bennett FC, Bohlen CJ, Schirmer L, Bennett ML, Münch AE, Chung WS, Peterson TC, et al. Neurotoxic reactive astrocytes are induced by activated microglia. Nature. 2017; 541:481–487. [PubMed: 28099414]

Lim KL, Ng XH, Grace LG, Yao TP. Mitochondrial dynamics and Parkinson's disease: focus on parkin. Antioxid Redox Signal. 2012; 16:935–49. [PubMed: 21668405]

Lin DC, Bullock CM, Ehlert FJ, Chen JL, Tian H, Zhou QY. Identification and molecular characterization of two closely related G protein-coupled receptors activated by prokineticins/endocrine gland vascular endothelial growth factor. J Biol Chem. 2002; 277:19276–80. [PubMed: 11886876]

Livak KJ, Schmittgen TD. Analysis of relative gene expression data using real-time quantitative PCR and the 2(-Delta Delta C(T)) Method. Methods. 2001; 25:402–8. [PubMed: 11846609]

Martucci C, Franchi S, Giannini E, Tian H, Melchiorri P, Negri L, Sacerdote P. Bv8, the amphibian homologue of the mammalian prokineticins, induces a proinflammatory phenotype of mouse macrophages. Br J Pharmacol. 2006; 147:225–34. [PubMed: 16299550]

Melchiorri D, Bruno V, Besong G, Ngomba RT, Cuomo L, De Blasi A, Copani A, Moschella C, Storto M, Nicoletti F, et al. The mammalian homologue of the novel peptide Bv8 is expressed in the central nervous system and supports neuronal survival by activating the MAP kinase/PI-3-kinase pathways. Eur J Neurosci. 2001; 13:1694–702. [PubMed: 11359521]

Miklossy J, Doudet DD, Schwab C, Yu S, McGeer EG, McGeer PL. Role of ICAM-1 in persisting inflammation in Parkinson disease and MPTP monkeys. Exp Neurol. 2006; 197:275–83. [PubMed: 16336966]

Monnier J, Samson M. Cytokine properties of prokineticins. Febs j. 2008; 275:4014–21. [PubMed: 18647349]

Morales I, Rodriguez M. Self-induced accumulation of glutamate in striatal astrocytes and basal ganglia excitotoxicity. Glia. 2012; 60:1481–94. [PubMed: 22715058]

Morrison HW, Filosa JA. A quantitative spatiotemporal analysis of microglia morphology during ischemic stroke and reperfusion. J Neuroinflammation. 2013; 10:4. [PubMed: 23311642]

Motori E, Puyal J, Toni N, Ghanem A, Angeloni C, Malaguti M, Cantelli-Forti G, Berninger B, Conzelmann KK, Gotz M, et al. Inflammation-induced alteration of astrocyte mitochondrial dynamics requires autophagy for mitochondrial network maintenance. Cell Metab. 2013; 18:844–59. [PubMed: 24315370]

Ng KL, Li JD, Cheng MY, Leslie FM, Lee AG, Zhou QY. Dependence of olfactory bulb neurogenesis on prokineticin 2 signaling. Science. 2005; 308:1923–7. [PubMed: 15976302]

Orihuela R, McPherson CA, Harry GJ. Microglial M1/M2 polarization and metabolic states. Br J Pharmacol. 2016; 173:649–65. [PubMed: 25800044]

Pekny M, Pekna M. Astrocyte reactivity and reactive astrogliosis: costs and benefits. Physiol Rev. 2014; 94:1077–98. [PubMed: 25287860]

Quirié A, Demougeot C, Bertrand N, Mossiat C, Garnier P, Marie C, Prigent-Tessier A. Effect of stroke on arginase expression and localization in the rat brain. Eur J Neurosci. 2013; 37:1193–202. [PubMed: 23311438]

Rappold PM, Tieu K. Astrocytes and therapeutics for Parkinson's disease. Neurotherapeutics. 2010; 7:413–23. [PubMed: 20880505]

Sattler R, Rothstein JD. Regulation and dysregulation of glutamate transporters. Handb Exp Pharmacol. 2006:277–303. [PubMed: 16722241]

Saura J, Pares M, Bove J, Pezzi S, Alberch J, Marin C, Tolosa E, Marti MJ. Intranigral infusion of interleukin-1beta activates astrocytes and protects from subsequent 6-hydroxydopamine neurotoxicity. J Neurochem. 2003; 85:651–61. [PubMed: 12694391]

Schweitz H, Pacaud P, Diochot S, Moinier D, Lazdunski M. MIT(1), a black mamba toxin with a new and highly potent activity on intestinal contraction. FEBS Lett. 1999; 461:183–8. [PubMed: 10567694]

Author Manuscript Author Manuscript Author Manuscript Author Manuscript

Swanson RA, Liu J, Miller JW, Rothstein JD, Farrell K, Stein BA, Longuemare MC. Neuronal regulation of glutamate transporter subtype expression in astrocytes. J Neurosci. 1997; 17:932–40. [PubMed: 8994048]

Tang Y, Le W. Differential Roles of M1 and M2 Microglia in Neurodegenerative Diseases. Mol Neurobiol. 2016; 53:1181–94. [PubMed: 25598354]

Teismann P, Tieu K, Cohen O, Choi DK, Wu DC, Marks D, Vila M, Jackson-Lewis V, Przedborski S. Pathogenic role of glial cells in Parkinson's disease. Mov Disord. 2003; 18:121–9. [PubMed: 12539204]

Urayama K, Guilini C, Messaddeq N, Hu K, Steenman M, Kurose H, Ert G, Nebigil CG. The prokineticin receptor-1 (GPR73) promotes cardiomyocyte survival and angiogenesis. Faseb J. 2007; 21:2980–93. [PubMed: 17442730]

Van Laar VS, Berman SB. The interplay of neuronal mitochondrial dynamics and bioenergetics: implications for Parkinson's disease. Neurobiol Dis. 2013; 51:43–55. [PubMed: 22668779]

Vargas MR, Johnson DA, Sirkis DW, Messing A, Johnson JA. Nrf2 activation in astrocytes protects against neurodegeneration in mouse models of familial amyotrophic lateral sclerosis. J Neurosci. 2008; 28:13574–81. [PubMed: 19074031]

Vellani V, Colucci M, Lattanzi R, Giannini E, Negri L, Melchiorri P, McNaughton PA. Sensitization of transient receptor potential vanilloid 1 by the prokineticin receptor agonist Bv8. J Neurosci. 2006; 26:5109–16. [PubMed: 16687502]

Volobouéva LA, Suh SW, Swanson RA, Giffard RG. Inhibition of mitochondrial function in astrocytes: implications for neuroprotection. J Neurochem. 2007; 102:1383–94. [PubMed: 17488276]

Wakabayashi K, Toyoshima Y, Awamori K, Anezaki T, Yoshimoto M, Tsuji S, Takahashi H. Restricted occurrence of Lewy bodies in the dorsal vagal nucleus in a patient with late-onset parkinsonism. J Neurol Sci. 1999; 165:188–91. [PubMed: 10450807]

Watson RP, Lilley E, Panesar M, Bhalay G, Langridge S, Tian SS, McClenaghan C, Ropenga A, Zeng F, Nash MS. Increased prokineticin 2 expression in gut inflammation: role in visceral pain and intestinal ion transport. Neurogastroenterol Motil. 2012; 24:65–75. e12. [PubMed: 22050240]

Yao HH, Ding JH, Zhou F, Wang F, Hu LF, Sun T, Hu G. Enhancement of glutamate uptake mediates the neuroprotection exerted by activating group II or III metabotropic glutamate receptors on astrocytes. J Neurochem. 2005; 92:948–61. [PubMed: 15686497]

Yasuda Y, Shimoda T, Uno K, Tateishi N, Furuya S, Yagi K, Suzuki K, Fujita S. The effects of MPTP on the activation of microglia/astrocytes and cytokine/chemokine levels in different mice strains. J Neuroimmunol. 2008; 204:43–51. [PubMed: 18817984]

Zamanian JL, Xu L, Foo LC, Nouri N, Zhou L, Giffard RG, Barres BA. Genomic analysis of reactive astrogliosis. J Neurosci. 2012; 32:6391–410. [PubMed: 22553043]

Zhou QY. The prokineticins: a novel pair of regulatory peptides. Mol Interv. 2006; 6:330–8. [PubMed: 17200460]

Zhou QY, Cheng MY. Prokineticin 2 and circadian clock output. Febs J. 2005; 272:5703–9. [PubMed: 16279936]

Zhou W, Li JD, Hu WP, Cheng MY, Zhou QY. Prokineticin 2 is involved in the thermoregulation and energy expenditure. Regul Pept. 2012; 179:84–90. [PubMed: 22960406]

Author Manuscript Author Manuscript Author Manuscript Author Manuscript

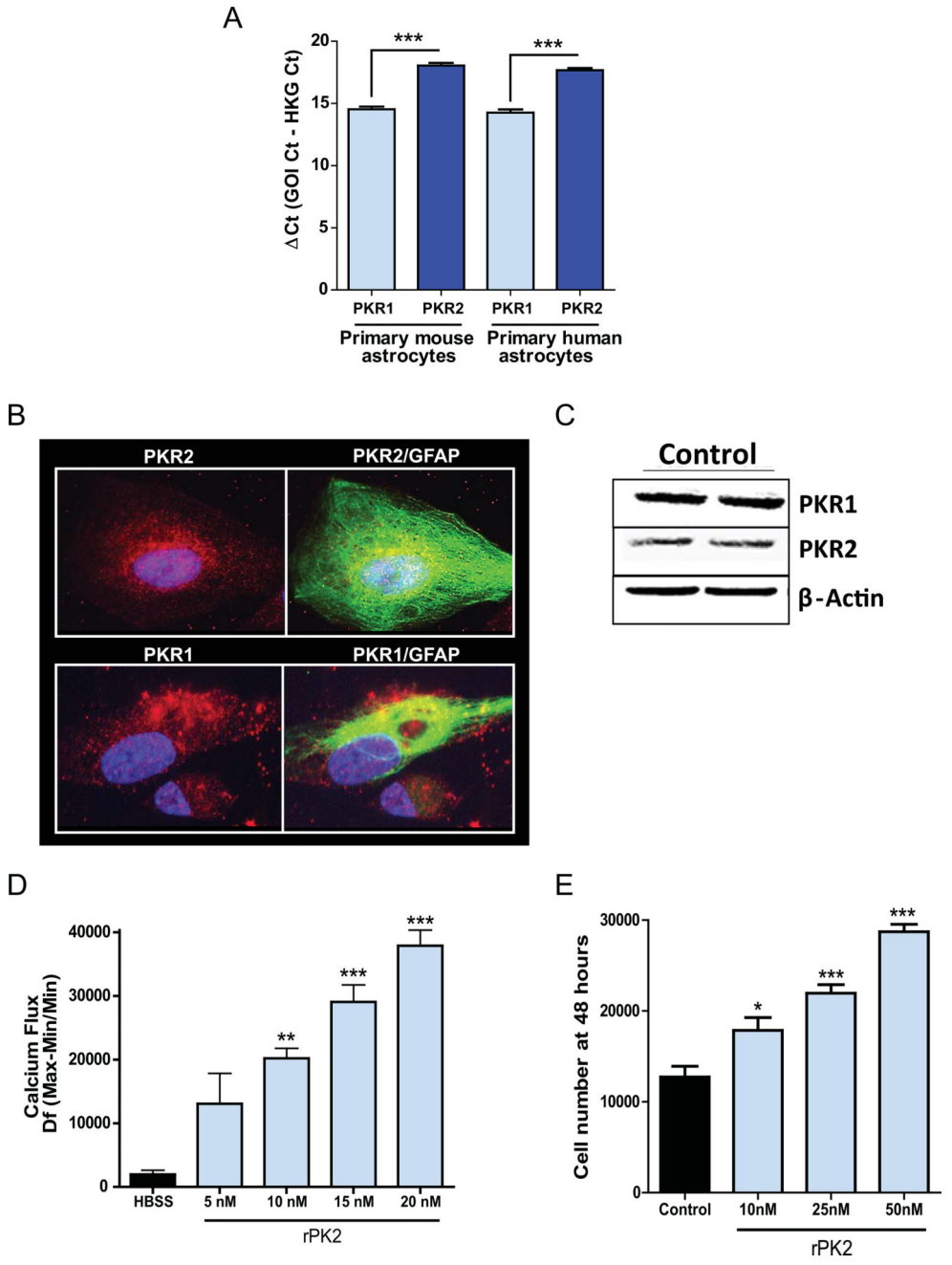

Figure 1. Prokineticin-2 treatment increases intracellular calcium and cell proliferation in primary mouse astrocytes

(**A**) Quantitative real time PCR for prokineticin receptor gene expression, with PKR1 expressed over 12-fold higher than PKR2. GOI: gene of interest; HKG: housekeeping gene. (**B**) Different cellular localization patterns for PKR2 (Red, top panel) and PKR1 (Red, bottom panel) in GFAP-positive (Green) astrocytes with the nucleus stained with Hoechst (Blue). Expression of PKR2 was peri-nuclear, whereas PKR1 expression was localized more to the cell periphery. (**C**) Representative Western blot for PKR1 and PKR2 in primary mouse astrocytes showing higher PKR1 (45 kDa) compared to PKR2 (44 kDa). (**D**) Calcium

Author Manuscript Author Manuscript Author Manuscript Author Manuscript

mobilization (flux) dose-dependently induced by rPK2 in primary mouse astrocytes, with calcium-free HBSS used as a control treatment. (**E**) CyQUANT cell proliferation assay used to show dose-dependent increase in primary mouse astrocyte cell proliferation. Asterisks denote a significant difference between rPK2 treatment and control (* $p<0.05$, ** $p<0.01$, and *** $p<0.001$).

Author Manuscript Author Manuscript Author Manuscript Author Manuscript

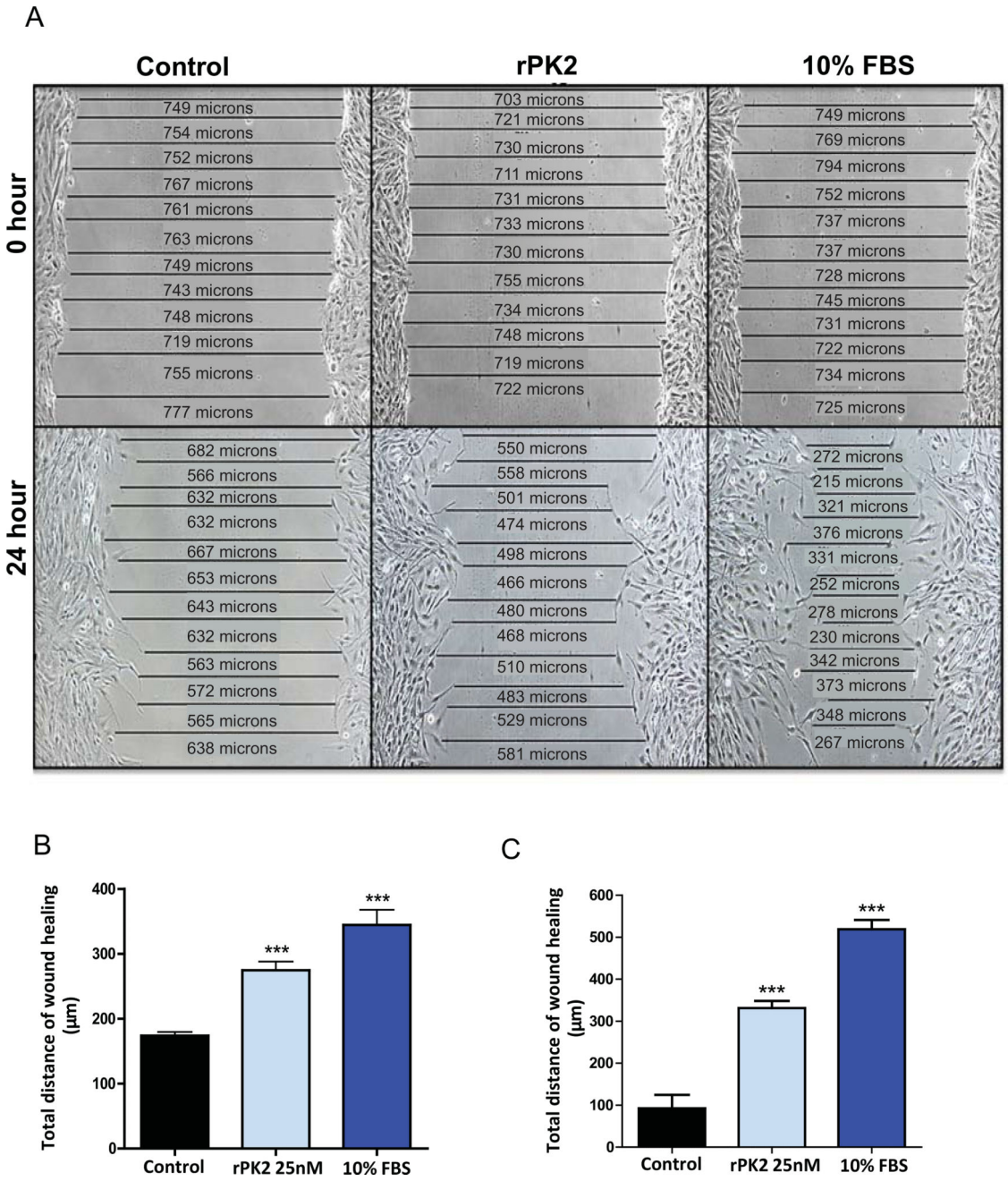

Figure 2. Recombinant PK2 treatment induces astrocyte wound healing

(**A**) Scratch-wound assay images for control, rPK2 and 10% FBS as a positive control from 0 h (top panel) and 24 h post-scratch (bottom panel) with multiple scale bars inserted at somewhat regular intervals along the scratch to measure wound width. (**B–C**) Analysis of total migration distance travelled from 0 h to 24 h showing that rPK2 treatment increased wound healing in the U373 human astrocyte cell line (B) and in normal human astrocytes (NHA) (C). Experiment was repeated twice with three biological replicates in each treatment. Asterisks denote statistically significant differences between treatments and control (*** $p<0.001$).

Author Manuscript Author Manuscript Author Manuscript Author Manuscript

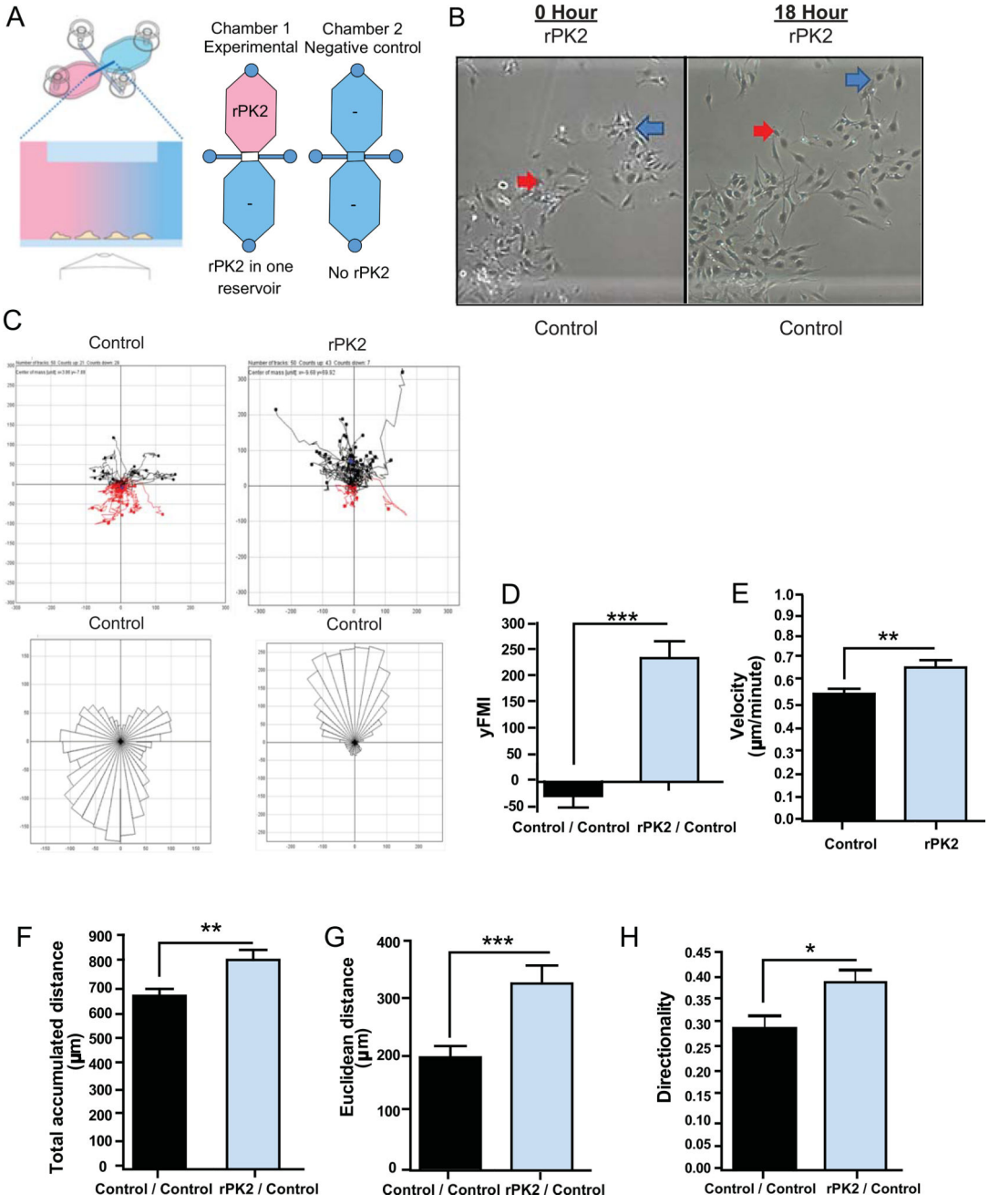

Figure 3. Prokineticin-2 induces astrocyte migration

(**A**) Ibidi 2D migration chamber setup to demonstrate experimental design for testing a chemoattractant by measuring directional migration of cells. (**B**) Phase contrast images from 0 h (left panel) and 18 h (right panel) after addition of PK2 treatment to the reservoir at the top of the image. Two different U373 cells are marked (red and blue arrows) both at 0 h and 18 h. (**C**) Migration tracking plots of individual cell migration tracks with either control (left panel) or PK2-treated (right panel) platforms, along with a rose plot for the migration tracks (bottom panels). (**D–H**) Analysis of the 2D migration chambers comparing control and PK2-treated platforms. Measurement for the single cell y-axis forward migration index (D),

migration velocity (E), total accumulated migration distance (F), Euclidean migration distance (G), and migration directionality (H), with all showing that PK2 significantly increased the directional migration of U373 astrocytes. Measurements were performed on at least 50 cells per treatment group, and asterisks denote statistically significant differences between the PK2 and control treatments (* $p<0.05$, ** $p<0.01$, and *** $p<0.001$).

Author Manuscript Author Manuscript Author Manuscript Author Manuscript

Author Manuscript Author Manuscript Author Manuscript Author Manuscript

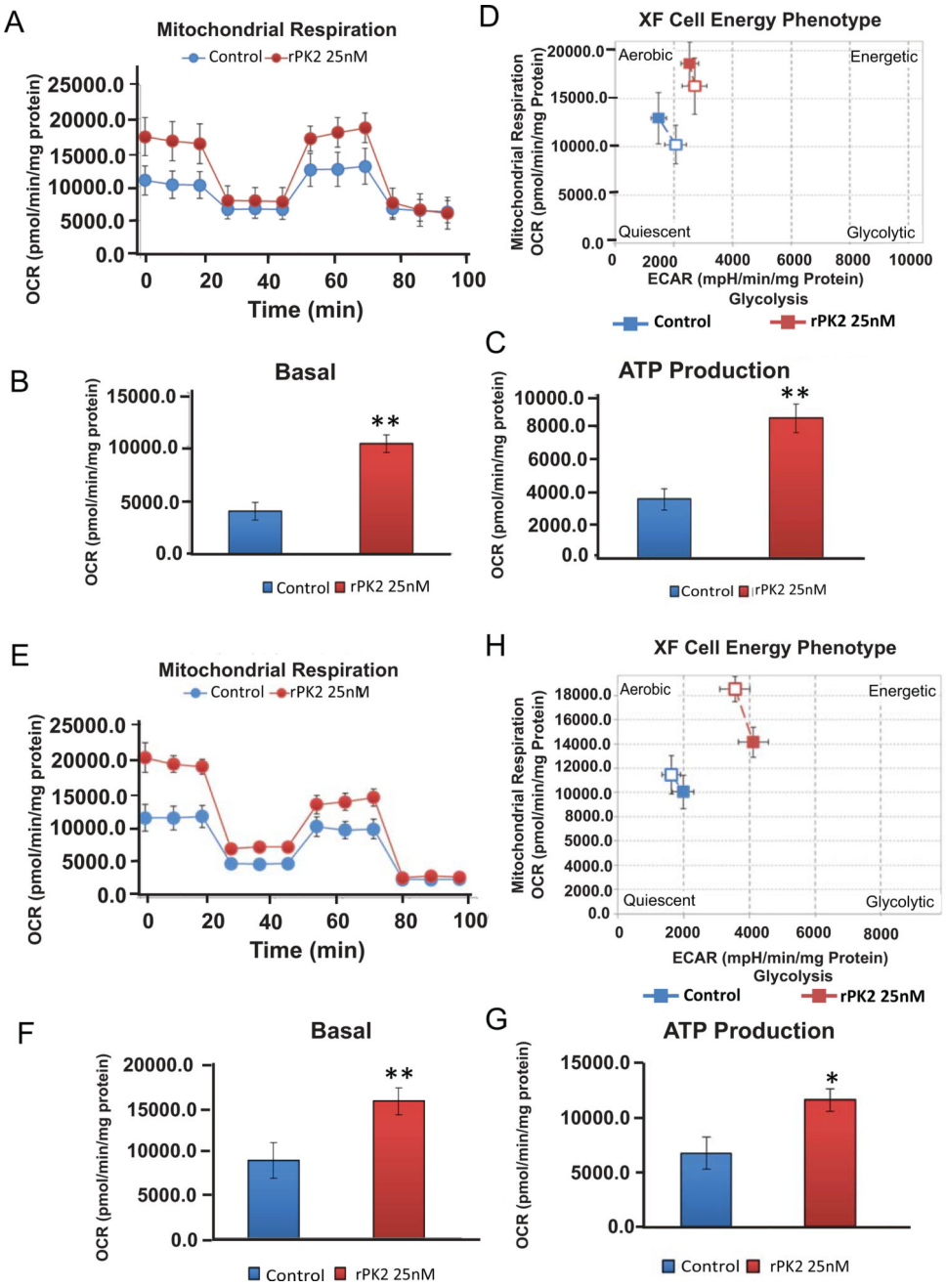

Figure 4. PK2 induces shift in mitochondrial dynamics and energy production

XFe24 Seahorse mitochondrial stress test on primary mouse astrocytes (A–D) and the U373 human astrocyte cell line (E–H). Analysis of mitochondrial respiration rate with the respiration plot (A and E), basal respiration (B and F) and ATP production (C and G) showing that PK2 treatment significantly induced oxidative respiration in astrocytes. Cellular phenotype plot comparing OCR on the y-axis and ECAR on the x-axis (D and H) shows that PK2 treatment increased overall energy production in primary mouse astrocytes and the U373 human astrocyte cell line. At least four biological replicates per treatment and

Author Manuscript Author Manuscript Author Manuscript Author Manuscript

experiments were repeated at least two times. Asterisks denote statistically significant differences between PK2 and control treatments (* $p<0.05$, and ** $p<0.01$).

Author Manuscript Author Manuscript Author Manuscript Author Manuscript

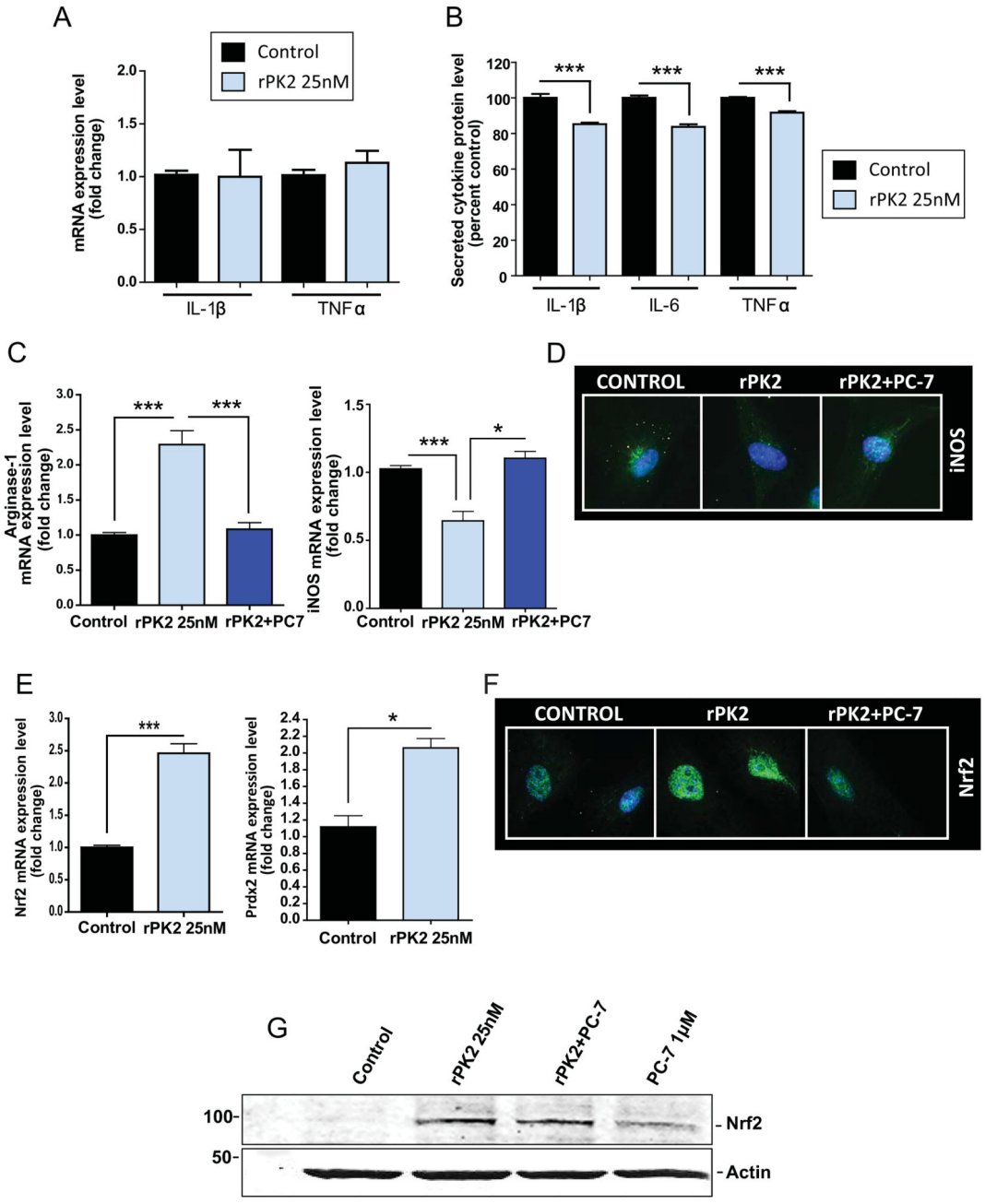

Figure 5. PK2 induces A1 to A2 conversion of astrocytic phenotype

(**A**) Quantitative real-time PCR analysis for the pro-inflammatory cytokines IL-1β and TNFα. (**B**) Pro-inflammatory cytokine protein levels measured in the primary mouse astrocyte conditioned media using the Bio-Plex 200 multiplex system for IL-1β, IL-6, and TNFα. (**C–D**) Recombinant PK2 treatment increased anti-oxidant factors in primary mouse astrocytes. (C) Quantitative real-time PCR analysis for arginase-1 (Left panel) and iNOS (Right panel). (D) Fluorescence microscopy images of iNOS protein level. (**E–F**) Recombinant PK2 treatment increased anti-oxidant factors in primary mouse astrocytes. (E) Quantitative real-time PCR gene expression analysis for Nrf2 (Left panel) and Prdx2 (Right

panel). (F) Fluorescence microscopy images detecting Nrf2 protein levels. (**G**) Western blot analysis for Nrf2 shows that PK2 treatment increased Nrf2 (110 kDa) protein level, whereas PC-7 attenuated this increase, with β-Actin (42 kDa) as an internal loading control. At least three biological replicates per treatment and experiments were repeated at least two times.

Author Manuscript Author Manuscript Author Manuscript Author Manuscript

Author Manuscript Author Manuscript Author Manuscript Author Manuscript

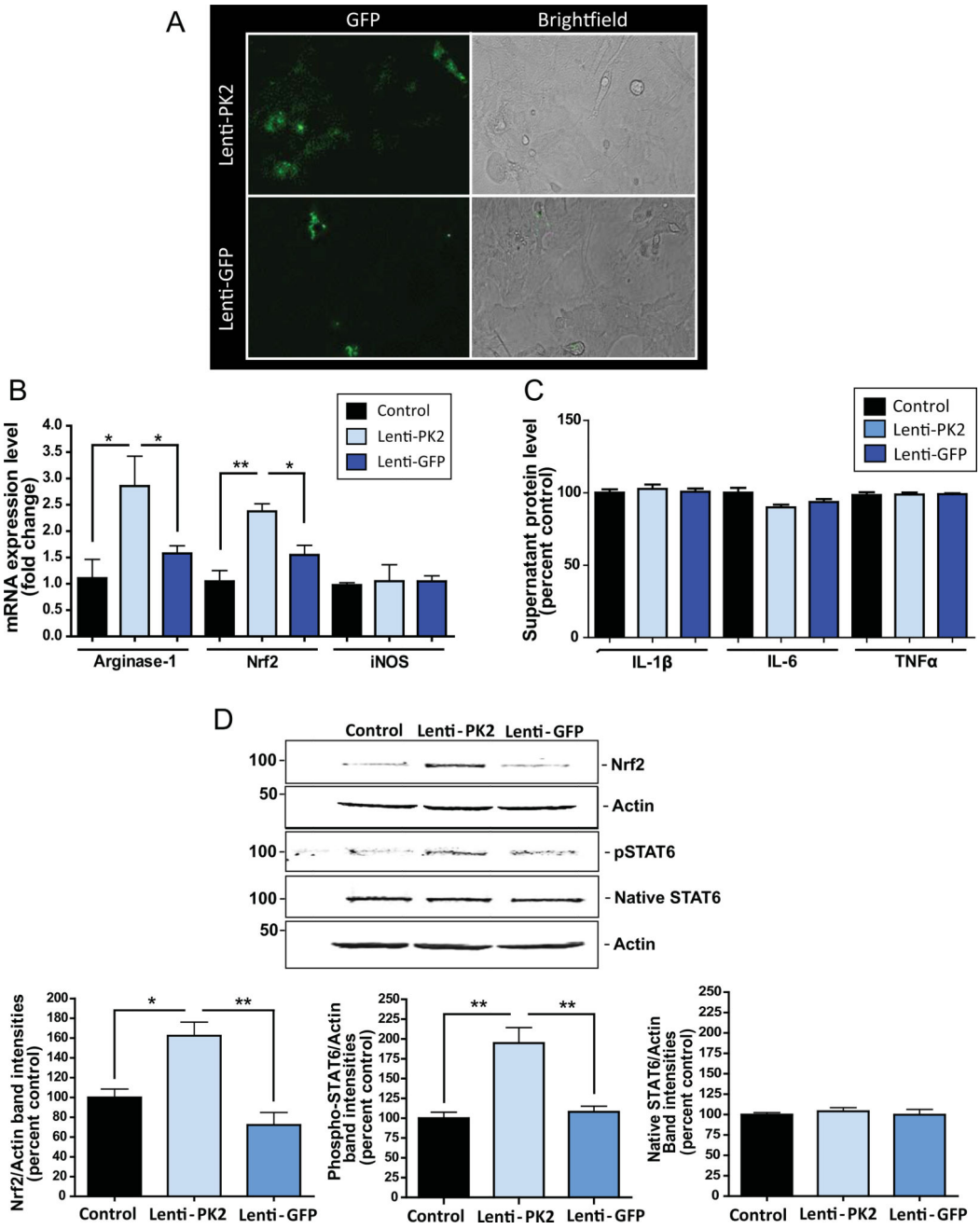

Figure 6. PK2 overexpression promotes alternative reactivity of astrocytes

(**A**) Fluorescence microscopy detected GFP, confirming lentiviral overexpression of PK2. (**B**) Quantitative real-time PCR gene expression analysis for arginase-1, Nrf2 and iNOS with PK2 overexpression. (C) Pro-inflammatory cytokine protein levels measured in the primary mouse astrocyte conditioned media using the Bio-Plex 200 multiplex system for IL-1β, IL-6, and TNFα. (**D**) Western blot analysis of PK2 overexpression for Nrf2 (110 kDa), phosphorylated STAT6 (100 kDa) and native STAT6 (100 kDa), with β-Actin (42 kDa) as an internal loading control. Asterisks denote statistically significant differences between Lenti-PK2 cells and either control or Lenti-GFP cells (* $p<0.05$, ** $p<0.01$, and *** $p<0.001$). At

Author Manuscript Author Manuscript Author Manuscript Author Manuscript

least three biological replicates per treatment and experiments were repeated at least two times.

Author Manuscript Author Manuscript Author Manuscript Author Manuscript

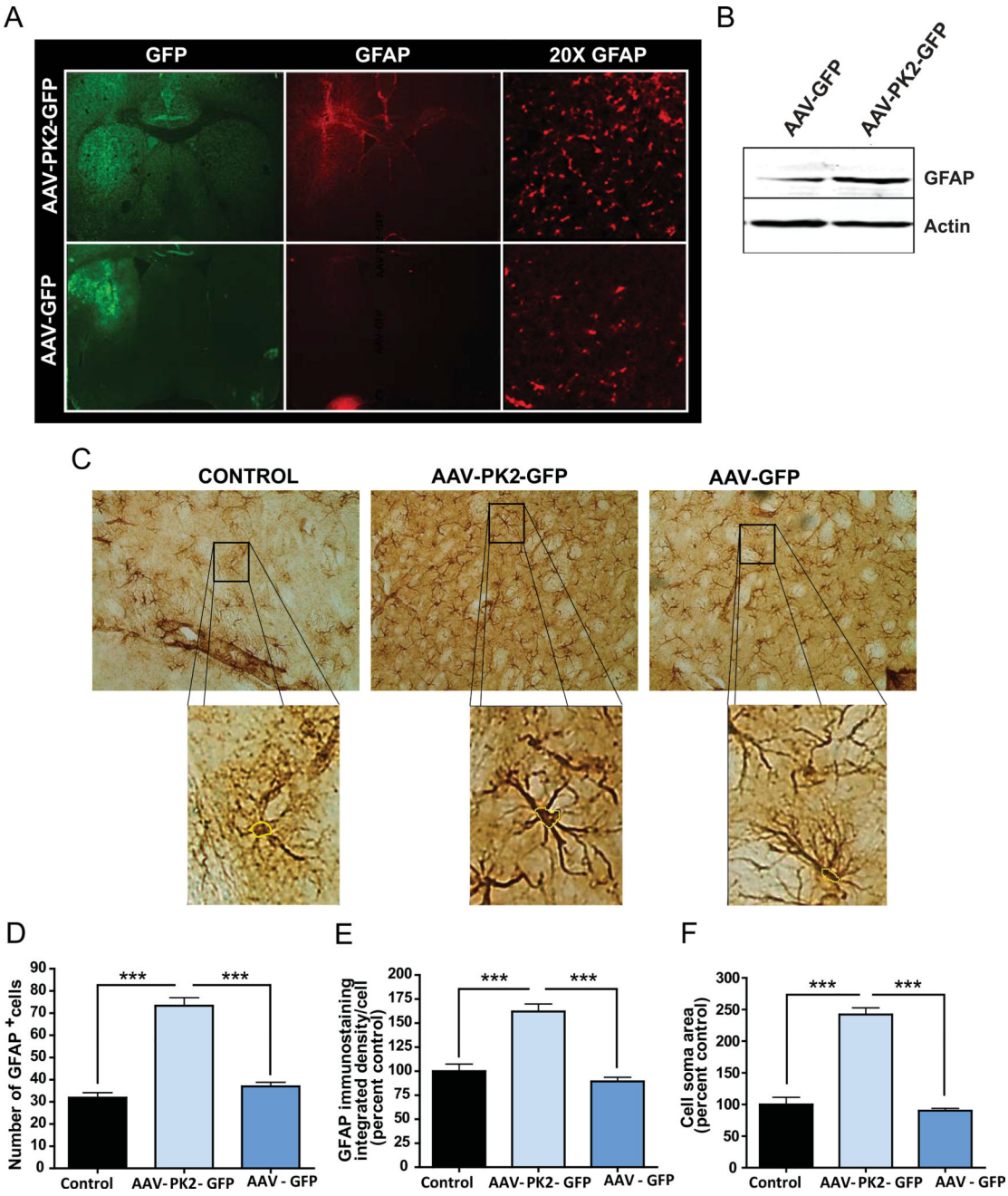

Figure 7. Prokineticin-2 overexpression induces astrocyte reactivity in vivo

C57BL/6 mice were stereotaxically injected in the striatum with either AAV 2/5-PK2-GFP or AAV 2/5-GFP and allowed four weeks to reach maximal viral gene expression. (**A**) Expression of the GFP-tagged PK2 and GFAP protein levels by fluorescence microscopy. Brain sections were probed with anti-GFP (Green) and anti-GFAP (Red) antibodies to show increased GFAP around the areas of GFP-tagged PK2 expression (2× left panel and 20× right panel). (**B**) Representative Western blot for GFAP (55 kDa) in the mouse striatum showing increased GFAP with the AAV-PK2-GFP, with β-Actin (42 kDa) as an internal loading control. (**C**) GFAP-DAB immunostaining of the striatum (20× top panel) with insets

zoomed into one cell. (**D**–**F**) Cell counting of GFAP-positive cells (D), immunostaining quantification of GFAP for each cell (E) and cell soma size of GFAP-positive cells (F) in the mouse striatum showing that AAV-PK2-GFP increased the number of GFAP-positive cells, the amount of GFAP, and cell soma size in these cells compared to AAV-GFP-injected and control striata. At least three biological replicates per treatment and experiments were repeated at least two times.

Author Manuscript Author Manuscript Author Manuscript Author Manuscript

Author Manuscript Author Manuscript Author Manuscript Author Manuscript

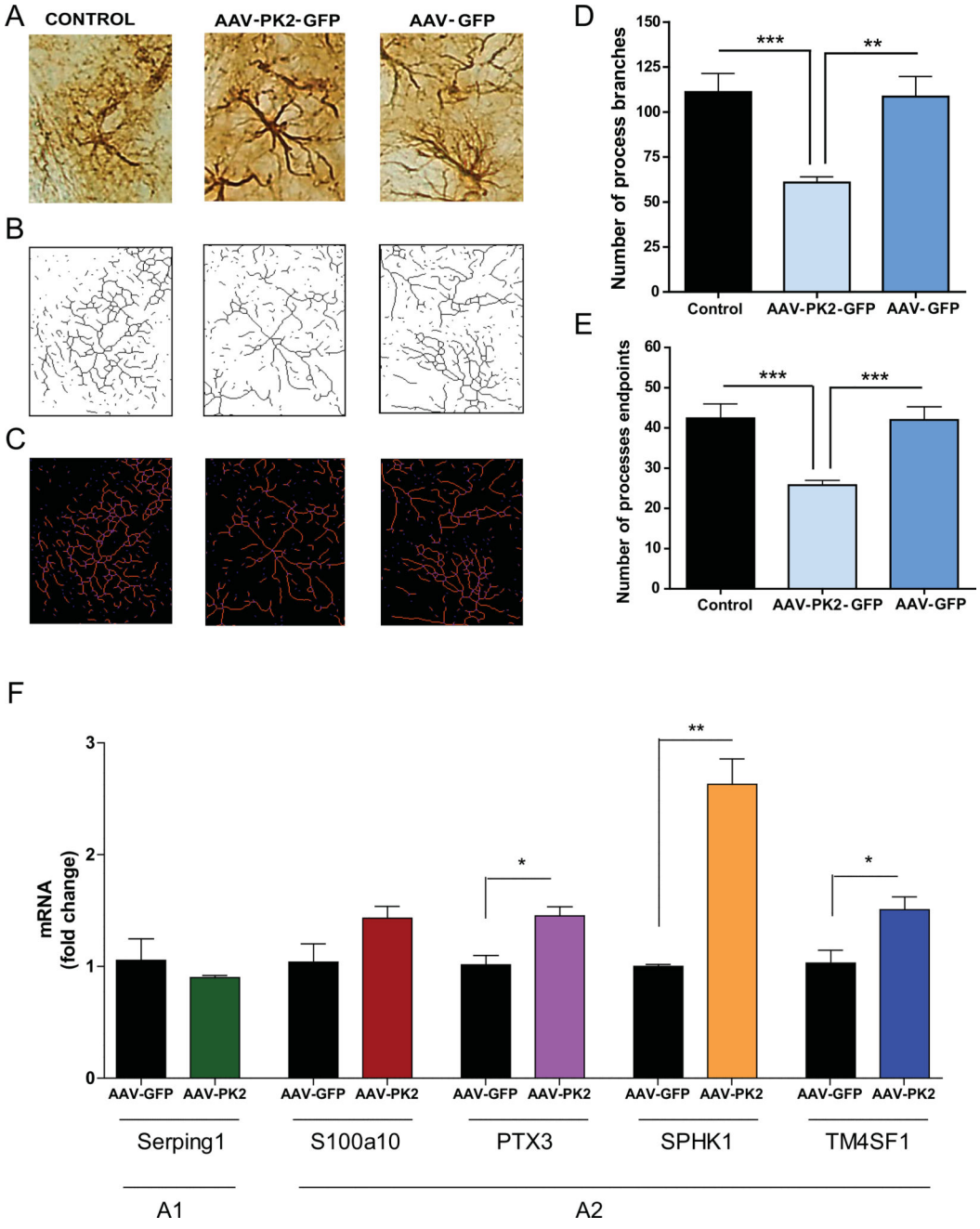

Figure 8. Prokineticin-2 overexpression reduces the number of astrocyte processes and promotes alternative reactivity in vivo

(**A–C**) Converting GFAP-DAB images for measurement of astrocyte processes after AAV-PK2-GFP or AAV-GFP injection in the striatum. (A) GFAP-DAB immunostaining for a control, AAV-PK2-GFP- and AAV-GFP-injected striatum (zoomed in images from 20× magnification). (B) ImageJ skeletonization after converting the GFAP-DAB image to a binary image. (C) ImageJ analyzed skeleton plug-in image from the skeletonized image with process branches (Orange), junctions (Purple), and endpoints (Blue). (**D–E**) Measurement of the astrocyte processes. Analysis for the average number of process branches (D) and process endpoints (E) per GFAP-positive astrocyte shows that AAV-PK2-GFP significantly

reduced the average number of cell process branches compared to control and AAV-GFP. (**F**) Real-Time qPCR of A1-specific gene Serping1 and A2-specific genes S100a10, PTX3, SPHK1, and TM4SF1. (* $p<0.05$). At least two biological replicates per treatment and experiments were repeated at least two times.

Author Manuscript Author Manuscript Author Manuscript Author Manuscript

Author Manuscript Author Manuscript Author Manuscript Author Manuscript

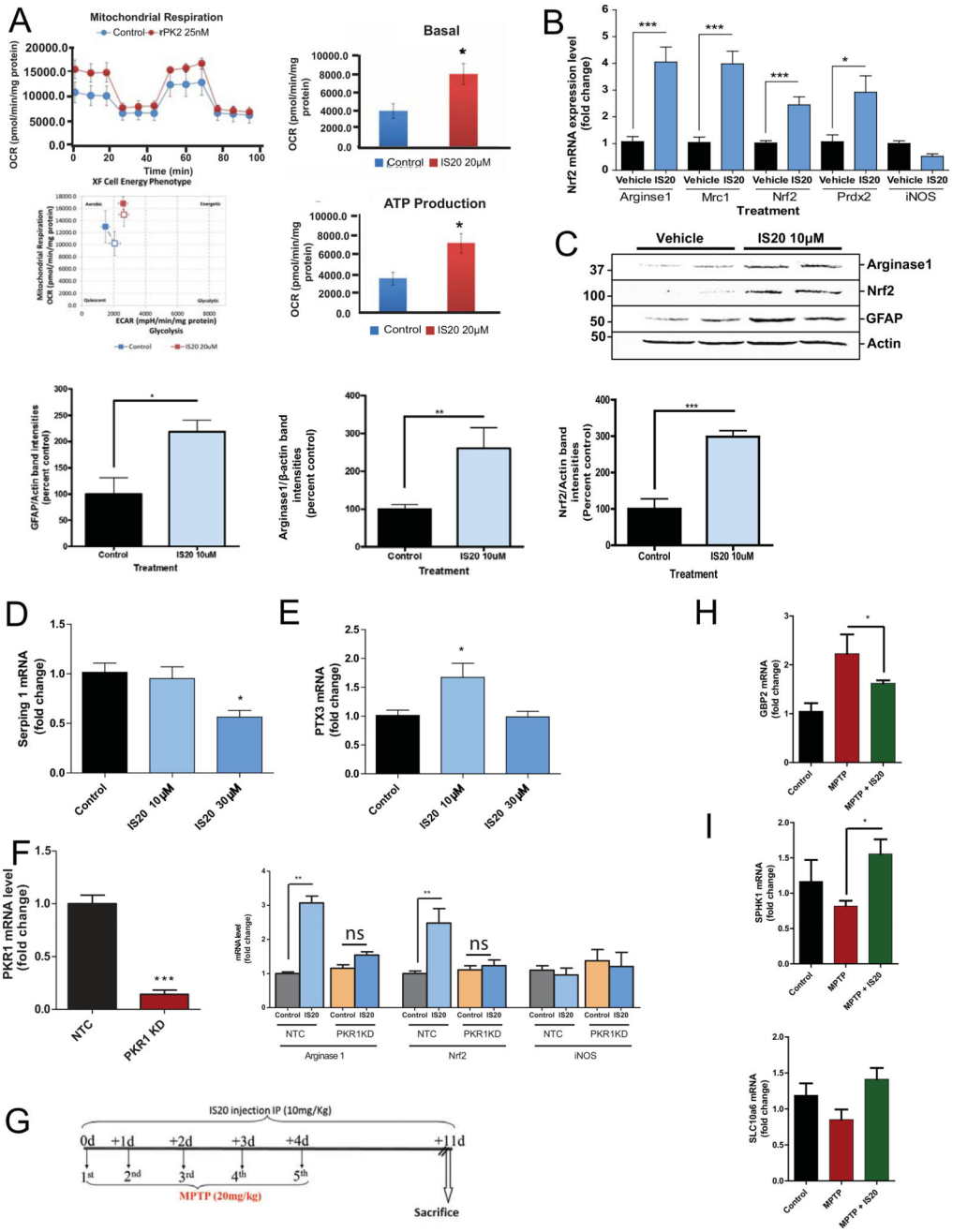

Figure 9. PKR1 agonist promotes alternative reactivity of primary mouse astrocytes

(**A**) Mitochondrial dynamics measured via the XFe24 Seahorse mitochondrial stress test (left panel) to compare IS20 to control for basal respiration and ATP production (middle panels). Cell energy phenotype plot (right panel) comparing OCR (y-axis) and ECAR (x-axis) shows that IS20 shifted astrocyte mitochondria to a more energetic phenotype. (**B**) Quantitative real-time PCR gene expression analysis for arginase1, Mrc1, Nrf2, Prdx2 and iNOS with IS20 treatment compared to control. (**C**) Western blot analysis for arginase1 (40 kDa) and Nrf2 (110 kDa) comparing IS20 treatment and control, with β-Actin (42 kDa) as an internal loading control. Asterisks denote statistically significant differences between IS20 treatment

Author Manuscript Author Manuscript Author Manuscript Author Manuscript

and control (* $p<0.05$, ** $p<0.01$, and *** $p<0.001$). Real-Time qPCR of **(D)** Serping1 and **(E)** PTX3. **(F)** CRISPR/Cas9-based knockdown of PKR1 in U373 cells infected with CRISPR/Cas9 PKR1 KD lentivirus or CRISPR/Cas9 non-target control (NTC) lentivirus. PKR1 expression was analyzed by real time qRT-PCR (Left panel). CRISPR/Cas9 PKR1 KD or CRISPR/Cas9 NTC-infected U373 cells were treated with or without 10 μM IS20. Arginase 1, Nrf2 and iNOS mRNA expression was analyzed by real time qRT-PCR (Right panel). ns, not significant. (**G**) Treatment paradigm of MPTP intraperitoneal injection in C57 black mice. Real-Time qPCR of (**H**) GBP2 and **(I)** SPHK1 and SLC10a6. At least three biological replicates per treatment and experiments were repeated at least two times.

Author Manuscript Author Manuscript Author Manuscript Author Manuscript

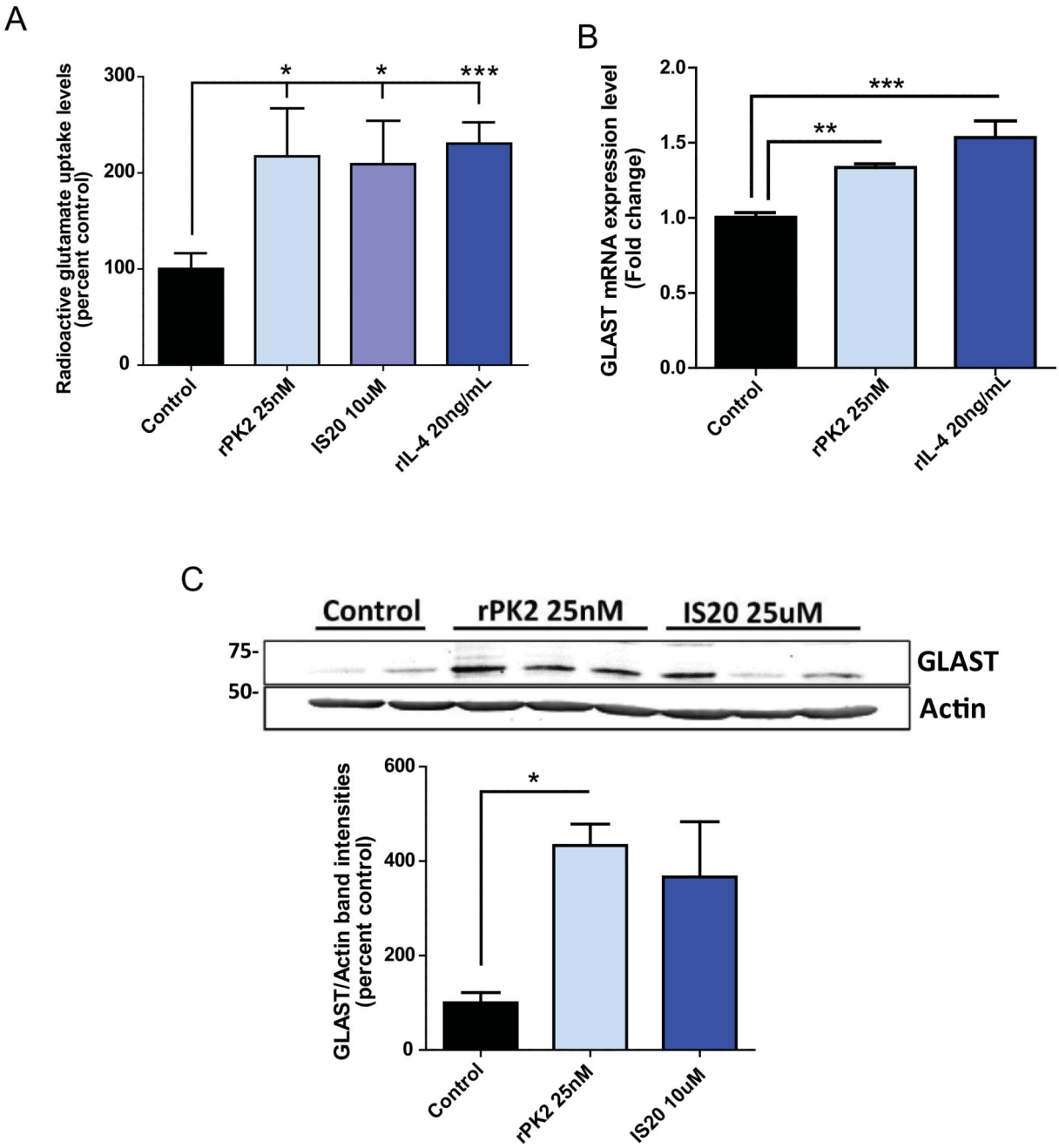

Figure 10. Prokineticin signaling increases glutamate uptake in cultured astrocytes through induction of GLAST gene expression

(**A**) Exogenously added radioactive glutamate levels in primary mouse astrocytes. (**B**) Quantitative real-time PCR gene expression analysis for GLAST with PK2 and IL-4 treatment compared to control. (**C**) Representative Western blot analysis for GLAST (60 kDa) protein level after treatment with PK2 and IS20, with β-Actin (42 kDa) as an internal loading control. Asterisks denote statistically significant differences between PK2, IS20 or IL-4 treatment and control (* $p<0.05$, ** $p<0.01$, and *** $p<0.001$). At least three biological replicates per treatment and experiments repeated at least two times.